Asymptotic bounds on the optimal radius when covering a set with minimum radius identical balls*

Ernesto G. Birgin† John L. Gardenghi‡ Antoine Laurain§

April 18, 2022

Abstract

The problem of covering a two-dimensional bounded set with a fixed number of minimum-radius identical balls is studied in the present work. An asymptotic expansion and bounds on the optimal radius as the number of balls goes to infinity are obtained for a certain class of nonsmooth domains. The proof is based on the approximation of the set to be covered by hexagonal honeycombs, and on the thinnest covering property of the regular hexagonal lattice arrangement in the whole plane. The dependence of the optimal radius on the number of balls is also investigated numerically using a shape optimization approach, and theoretical and numerical convergence rates are compared. An initial point construction strategy is introduced which, in the context of a multi-start method, finds good quality solutions to the problem under consideration. Extensive numerical experiments with a variety of polygonal regions and regular polygons illustrate the introduced approach.

Keywords: Covering with balls, asymptotic bounds, shape optimization, numerical optimization.

AMS subject classification: 49Q10, 49J52, 49Q12

1 Introduction

The problems of covering bounded sets or the whole space with balls, in any dimension, have been extensively studied in the literature. A mathematical investigation of such a problem seems to appear for the first time in a paper of Neville in 1915 [30], where he illustrates a numerical method for solving systems of nonlinear equations with the problem of covering a disc by five smaller discs. Kershner [24] pioneered the topic in 1939, providing an asymptotic result on the smallest number of discs of fixed radius r that are necessary to cover an arbitrary region of the plane. This was followed by a series of works on lattice coverings starting from the paper of Fejes Tóth in 1948 [19], showing in particular that the disc is the least economical symmetrical convex plane set, from the

*This work has been partially supported by FAPESP (grants 2013/07375-0, 2016/01860-1, 2018/24293-0, and 2019/25258-7) and CNPq (grants 303243/2021-0, 302682/2019-8, 304258/2018-0, and 408175/2018-4).

†Department of Computer Science, Institute of Mathematics and Statistics, University of São Paulo, Rua do Matão, 1010, Cidade Universitária, 05508-090, São Paulo, SP, Brazil. e-mail: egbirgin@ime.usp.br

‡Faculty UnB Gama, University of Brasília, Área Especial de Indústria Projeção A, Setor Leste, Gama, 72444-240, Brasília, DF, Brazil. e-mail: john.gardenghi@unb.br

§Department of Applied Mathematics, Institute of Mathematics and Statistics, University of São Paulo, Rua do Matão, 1010, Cidade Universitária, 05508-090, São Paulo, SP, Brazil. e-mail: laurain@ime.usp.br

point of view of lattice coverings. Results of a similar nature were provided in 1952 by Bambah and Rogers [3] using a different method, including the problem of covering a convex set with convex sets. In 1950, Fáry studied lattice coverings with a plane convex set that is not necessarily symmetrical [18]. In 1954, Bambah studied thinnest lattice coverings by three-dimensional equal spheres [2]. Extensive work on the covering of a disc by smaller discs was done by Kahn Jr. [39] in 1962. In his work, approximating the area covered by a given configuration, Kahn Jr. set out to extensively test different optimization algorithms available. In a way, it is possible to say that Kahn Jr.'s work was a precursor to the many subsequent works that were devoted to the covering problem with the help of computer-aided strategies.

Proven optimal solutions for covering a unit-sided equilateral triangle with up to six identical discs were presented in [27], using simple plane geometry arguments. Another way to prove optimality of a solution is to show that it meets a known lower bound. A lower bound coming from known optimal solutions of the packing problem (known as the dual of the covering problem) is mentioned in [28, §4]. However, proven optimal solutions of the packing problem can also be calculated only for problems with few balls or specific symmetries, using plane geometry arguments. In this way, the optimality of some few-balls covering solutions has been proven. In the general case, in the last decades, a variety of computer-aided strategies were used to find presumably good quality solutions; see [5, 8, 9, 10, 20, 27, 28, 29, 31, 32]. As computational power increases and more efficient numerical methods emerge, covering problems with a large number of discs can be solved numerically. On the one hand, numerical experiments are then useful to gain insight and to verify properties of the solutions, such as the dependence of the optimal radius $r^*(m)$ and balls' centers on the number of balls m used for the covering. On the other hand, theoretical properties of the solutions help to limit the distance of a numerically calculated solution to an (unknown) optimal solution.

Among the properties of optimal coverings that can be investigated, understanding the behaviour of $r^*(m)$ as $m \to +\infty$ is of particular interest. The thinnest covering of the plane is achieved by arranging the discs' centers in a regular hexagonal lattice; see [15, Ch.2,p.32]. Thus, it is expected that, when covering an arbitrary given bounded set A, the optimal configuration of the discs' centers converges, in some sense, to such a regular hexagonal lattice as $m \to +\infty$. This allows in particular to obtain $\lim_{m\to\infty} r^*(m)\sqrt{m} = \left[2\,\mathrm{Vol}(A)/3\sqrt{3}\right]^{1/2}$, where $\mathrm{Vol}(A)$ is the area of A. These properties are observed numerically, and a similar asymptotic result was proved by Kershner [24] for the minimal number of identical discs with given radius required to cover an arbitrary bounded set. Kershner also provided lower and upper bounds for the covering of rectangles that was the basis for obtaining his asymptotic result; these bounds were improved by Verblunksy [37] for the particular case of a square of size σ covered by discs of unit radius and for sufficiently large σ. Various asymptotic results have also been obtained for similar problems such as the problem of seeking a convex set with maximal area that a given number of discs of fixed radius can cover. In this context, an important result is the Fejes-Tóth inequality, where an estimate for the area of a convex domain covered by m unit discs is given, see [13, Thm. 5.2.2]; see also [4, 6] for the covering of the convex hull of the discs' centers. More recently, [21] presented a lower bound on the sum of radii of small balls covering a unit d-dimensional Euclidean ball. The work also gives an upper bound on the sum of powers of the balls' radii.

Even though lower and upper bounds for $r^*(m)$ are available for specific geometries such as rectangles and spheres, refined asymptotic expansions that improve the results of Kershner for arbitrary domains seem to be lacking. In this paper we contribute to this task by providing an asymptotic expansion of $r^*(m)$ as $m \to +\infty$ for a relatively large class of sets to be covered. We start by discussing the relation between the problem considered by Kershner of finding the minimal number of identical discs with given radius required to cover an arbitrary bounded set and the problem of finding bounds for $r^*(m)$. We show indeed that $\lim_{m\to\infty} r^*(m)\sqrt{m} = \left[2\,\mathrm{Vol}(A)/3\sqrt{3}\right]^{1/2}$, and in addition we prove upper and lower bounds of order $2\,\mathrm{Per}(\partial A)/(3\sqrt{3}m)$ for the next term of the asymptotic expansion of $r^*(m)$. The methodology consists in trapping A between two hexagonal honeycombs with m cells, based on a regular hexagonal lattice arrangement of variable size, that converge in some sense towards A, and to use the thinnest covering property of the regular hexagonal lattice arrangement in the whole plane. The methodology of Kershner and Verblunksy to obtain the upper bound is also relying on a trapping of A, but using sets defined as unions of rectangles of different sizes. For the lower bounds, they use a different technique based on Voronoi cells.

From a practical point of view, we consider the shape optimization framework introduced in [9, 10] to produce covers of polygonal sets. In [9, 10], using shape optimization techniques, first- and second-order derivatives of a nonlinear programming (NLP) model of the problem were computed. With these tools, an NLP method was combined with a rough random multi-start strategy to compute good quality coverings of varied polygonal sets. In the present work, based on the obtained optimal solutions' theoretical properties, we introduce a strategy to construct randomized lattice-like starting points for the optimization process. In this way, we make an enhancement of the multi-start strategy, which ends up needing many fewer attempts to find good quality solutions. This computational tool is then used to assert the optimal solutions' theoretical properties. Additionally, solutions with up to one hundred balls for regular polygons are presented as an illustration.

The rest of this paper is organized as follows. In Section 2, the minimization problem based on a shape optimization approach is formulated, and the formulas for the first- and second-order derivatives of the constraint are given. In Section 3, the asymptotic expansion and bounds on $r^*(m)$ are given as $m \to \infty$ and compared with the results of Kershner. In Section 4, a methodology for the heuristic generation of lattice-based initial guesses is described. In Section 5, numerical experiments are conducted for various types of domains A. The theoretical rate of convergence of the bounds are compared to the numerical rate of convergence. Conclusions and lines for future research are given in the last section.

Notation: Given $x, y \in \mathbb{R}^n$, $x \cdot y = x^T y \in \mathbb{R}$, $x \otimes y = xy^T \in \mathbb{R}^{n\times n}$ and $\|x\|$ denotes the Euclidean norm. Given an open set S, $\overline{S}$ denotes its closure, S^c its complementary, and $\partial S = \overline{S} \setminus S$ denotes its boundary. For a two-dimensional set S, $\mathrm{Vol}(S)$ denotes its area, $\mathrm{Per}(\partial S)$ its perimeter and $d(x, S)$ the distance of a point x to S. For a closed set S, $\mathrm{int}\, S$ denotes its interior. For a finite set S, $|S|$ denotes its cardinal.

2 The shape optimization problem

Let $A \subset \mathbb{R}^2$ be an open set and $\Omega(\boldsymbol{x}, r) = \cup_{i=1}^m B(x_i, r)$, where $B(x_i, r)$ for $i = 1, \dots, m$ are open balls with centers $x_i \in \mathbb{R}^2$ and radii r and $\boldsymbol{x} := \{x_i\}_{i=1}^m$. We consider the problem of covering A using a fixed number m of balls $B(x_i, r)$ with minimum radius r, i.e., we are looking for $(\boldsymbol{x}, r) \in \mathbb{R}^{2m+1}$ such that $A \subset \Omega(\boldsymbol{x}, r)$ with minimum r. The problem can be formulated as

$$\underset{(\boldsymbol{x},r)\in\mathbb{R}^{2m+1}}{\text{Minimize}} \; r \;\text{ subject to }\; G(\boldsymbol{x}, r) = 0, \tag{1}$$

where

$$G(\boldsymbol{x}, r) := \mathrm{Vol}(A) - \mathrm{Vol}(A \cap \Omega(\boldsymbol{x}, r)). \tag{2}$$

Note that $G(\boldsymbol{x}, r) = 0$ if and only if $A \subset \Omega(\boldsymbol{x}, r)$ up to a set of zero measure, i.e., when $\Omega(\boldsymbol{x}, r)$ covers A.

Problem (1,2) was numerically solved in [9, 10] using the first and second derivatives of G, that were computed using techniques of shape calculus [17, 23, 25, 26, 33] under the following regularity assumptions.

Assumption 1. *The centers $\{x_i\}_{i=1}^m$ satisfy $\|x_i - x_j\| \notin \{0, 2r\}$ for $1 \le i, j \le m$, $i \ne j$ and $\partial B(x_i, r) \cap \partial B(x_j, r) \cap \partial B(x_k, r) = \emptyset$ for all $1 \le i, j, k \le m$ with i, j, k pairwise distinct.*

Definition 1. Let ω_1, ω_2 be open subsets of $\mathbb{R}^2$. We call ω_1 and ω_2 *compatible* if $\omega_1 \cap \omega_2 \ne \emptyset$, ω_1 and ω_2 are Lipschitz domains, and the following conditions hold: (i) $\omega_1 \cap \omega_2$ is a Lipschitz domain; (ii) $\partial\omega_1 \cap \partial\omega_2$ is finite; (iii) $\partial\omega_1$ and $\partial\omega_2$ are locally smooth in a neighborhood of $\partial\omega_1 \cap \partial\omega_2$; (iv) $\tau_1(x) \cdot \nu_2(x) \ne 0$ for all $x \in \partial\omega_1 \cap \partial\omega_2$, where $\tau_1(x)$ is a tangent vector to $\partial\omega_1$ at x and $\nu_2(x)$ is a normal vector to $\partial\omega_2$ at x.

Assumption 2. *Sets $\Omega(\boldsymbol{x}, r)$ and A are compatible.*

Under Assumptions 1 and 2 it was shown in [9] that

$$\nabla G(\boldsymbol{x}, r) = -\left(\int_{\mathcal{A}_1} \nu(z)\, dz, \cdots, \int_{\mathcal{A}_m} \nu(z)\, dz, \int_{\partial\Omega(\boldsymbol{x}, r) \cap A} dz \right)^{\top}, \tag{3}$$

where

$$\mathcal{A}_i = \partial B(x_i, r) \cap \partial\Omega(\boldsymbol{x}, r) \cap A, \tag{4}$$

and $\nu(z) \in \mathbb{R}^2$, in the ith component of (3), is the outward unit normal vector to $\mathcal{A}_i$ at z, for $i = 1, \dots, m$. Furthermore, under the same assumptions, in [10] it was shown that

$$\nabla^2 G(\boldsymbol{x}, r) = \begin{pmatrix} \nabla^2_{\boldsymbol{x}} G(\boldsymbol{x}, r) & \nabla^2_{\boldsymbol{x}, r} G(\boldsymbol{x}, r) \\ \nabla^2_{\boldsymbol{x}, r} G(\boldsymbol{x}, r)^{\top} & \nabla^2_r G(\boldsymbol{x}, r) \end{pmatrix}, \tag{5}$$

where $\nabla^2_{\boldsymbol{x}} G(\boldsymbol{x}, r) \in \mathbb{R}^{2m \times 2m}$, $\nabla^2_{\boldsymbol{x}, r} G(\boldsymbol{x}, r) \in \mathbb{R}^{2m}$, and $\nabla^2_r G(\boldsymbol{x}, r) = \partial^2_r G(\boldsymbol{x}, r) \in \mathbb{R}$ are described below.

Each arc in $\mathcal{A}_i$ can be represented by a pair of points (v, w), named starting and ending points, in counter-clockwise direction, i.e., such that the angular coordinates θ_v and θ_w of $v - x_i$ and $w - x_i$, respectively, satisfy $\theta_v \in [0, 2\pi)$ and $\theta_w \in (\theta_v, \theta_v + 2\pi]$. If $\mathcal{A}_i$ is not a full circle, we denote by $\mathbb{A}_i$ the set of pairs (v, w) that represent the arcs in $\mathcal{A}_i$; otherwise, we define $\mathbb{A}_i = \emptyset$. For a starting or ending point z of an arc in $\mathbb{A}_i$, let $L(z) = \{\ell \in \{1, \dots, m\} \setminus \{i\} \mid z \in \partial B(x_\ell, r)\}$, $\tau_i(z)$ be the unitary-norm tangent vector to $\partial B(x_i, r)$ at z (pointing counter-clockwise), $\nu_i(z)$ be the unitary-norm outwards normal vector to $\partial B(x_i, r)$ at z, and $\nu_{-i}(z)$ be the unitary-norm outwards normal vector to the set intersecting $\partial B(x_i, r)$ at z (it could be either ∂A or $\partial B(x_\ell, r)$ for $\ell \in L(z)$). We say a configuration $(\boldsymbol{x}, r)$ is *non-degenerate* if Assumptions 1 and 2 are satisfied in this configuration. This implies that for every $i = 1, \dots, m$, every $(v, w) \in \mathbb{A}_i$, and every $z \in \{v, w\}$, there exists one and only one $\nu_{-i}(z)$ and $\nu_{-i}(z) \cdot \tau_i(z) \ne 0$.

Assuming $(\boldsymbol{x}, r)$ is non-degenerate we have that $\nabla_r^2 G(\boldsymbol{x}, r)$ in (5) is given by

$$\nabla_r^2 G(\boldsymbol{x}, r) = -\frac{\operatorname{Per}(\partial\Omega(\boldsymbol{x}, r) \cap A)}{r} - \sum_{i=1}^{m} \sum_{(v,w)\in\mathbb{A}_i} \left[\!\!\left[\frac{|L(z)| - \nu_{-i}(z) \cdot \nu_i(z)}{\nu_{-i}(z) \cdot \tau_i(z)} \right]\!\!\right]_v^w, \tag{6}$$

where, for an arbitrary expression $\Phi(z)$, $[\![\Phi(z)]\!]_v^w := \Phi(w) - \Phi(v)$. Matrix $\nabla_{\boldsymbol{x}}^2 G(\boldsymbol{x}, r)$ in (5) is given by the 2×2 diagonal blocks

$$\partial^2_{x_i x_i} G(\boldsymbol{x}, r) = \frac{1}{r} \int_{\mathcal{A}_i} -\nu_i(z) \otimes \nu_i(z) + \tau_i(z) \otimes \tau_i(z)\, dz + \sum_{(v,w)\in\mathbb{A}_i} \left[\!\!\left[\frac{\nu_{-i}(z) \cdot \nu_i(z)}{\nu_{-i}(z) \cdot \tau_i(z)}\, \nu_i(z) \otimes \nu_i(z) \right]\!\!\right]_v^w \tag{7}$$

and the 2×2 off-diagonal blocks

$$\partial^2_{x_i x_\ell} G(\boldsymbol{x}, r) = \sum_{v \in \mathcal{I}_{i\ell}} \frac{\nu_i(v) \otimes \nu_\ell(v)}{\nu_\ell(v) \cdot \tau_i(v)} - \sum_{w \in \mathcal{O}_{i\ell}} \frac{\nu_i(w) \otimes \nu_\ell(w)}{\nu_\ell(w) \cdot \tau_i(w)}, \tag{8}$$

where $\mathcal{I}_{i\ell} = \{v \in \partial B(x_\ell, r) \mid (v, \cdot) \in \mathbb{A}_i\}$ and $\mathcal{O}_{i\ell} = \{w \in \partial B(x_\ell, r) \mid (\cdot, w) \in \mathbb{A}_i\}$. (Note that $\mathcal{I}_{i\ell} = \mathcal{O}_{i\ell} = \emptyset$ for all $\ell \neq i$ if $\mathbb{A}_i = \emptyset$.) Finally, array $\nabla^2_{\boldsymbol{x},r} G(\boldsymbol{x}, r)$ in (5) is given by the 2-dimensional arrays

$$\partial^2_{x_i r} G(\boldsymbol{x}, r) = -\frac{1}{r} \int_{\mathcal{A}_i} \nu_i(z)\, dz + \sum_{(v,w)\in\mathbb{A}_i} \left[\!\!\left[\frac{\nu_{-i}(z) \cdot \nu_i(z)}{\nu_{-i}(z) \cdot \tau_i(z)} \nu_i(z) - \sum_{\ell \in L(z)} \frac{\nu_i(z)}{\tau_i(z) \cdot \nu_\ell(z)} \right]\!\!\right]_v^w. \tag{9}$$

We conclude this section by mentioning that various singular cases where $(\boldsymbol{x}, r)$ is degenerate were analyzed in [9, 10]. On the one hand, it was shown that G is often differentiable and in the few cases where G is not differentiable it is at least Gateaux semidifferentiable. On the other hand, G is usually not twice differentiable when $(\boldsymbol{x}, r)$ is degenerate, but Gateaux semidifferentiability of the components of ∇G can often be proven. In any case, it was observed that these differentiability issues are not detrimental for the numerical algorithms developed in [9, 10], which were consistently able to find satisfactory solutions even in the most singular cases.

3 Asymptotic expansion of the optimal radius

In this section we provide an asymptotic expansion with respect to m, as $m \to +\infty$, of the optimal radius $r^*(m)$ solution to problem (1,2). The methodology consists in trapping A between a lower honeycomb H_1 and an upper honeycomb H_0, where the honeycombs are unions of m regular hexagons whose centers belong to a regular hexagonal lattice.

We start by discussing the differences between our results and the results of Kershner [24]. In [24], the problem of estimating the minimum number of identical discs of given radius r that is required to cover an arbitrary bounded set $A \subset \mathbb{R}^2$ is considered. This problem seems somehow dual to the problem that we consider in the present paper, but the two problems are actually not completely equivalent, at least for arbitrary bounded set $A \subset \mathbb{R}^2$. We discuss here the main differences and how the estimates obtained in [24] can be interpreted in the framework of the minimization problem (1,2).

We start by defining the class $\mathcal{S}$ of sets to be covered considered in the present paper. Note that the sets in $\mathcal{S}$ need not be Lipschitz, and may in particular include cracks and cusps.

Definition 2. Let $\mathcal{S}$ be the set of open and bounded sets $A \subset \mathbb{R}^2$ satisfying

$$\partial A = \bigcup_{k=1}^{\bar{k}} \overline{\Gamma_k}, \quad k = 1, \ldots, \bar{k}, \tag{10}$$

where Γ_k is a smooth open or closed arc, $\bar{k} < +\infty$, and $\overline{\Gamma_k} \cap \overline{\Gamma_j}$ is either empty or composed of one or two points, for all $j \neq k$, $j, k = 1, \ldots, \bar{k}$. Here $\bar{k}$ denotes the number of edges of A.

Let $N(r)$ be the minimal number of identical closed discs with given radius r required to cover a bounded set $A \subset \mathbb{R}^2$. The main result of [24] states that

$$\lim_{r \to 0} \pi r^2 N(r) = \frac{2\pi\sqrt{3}\,\mathrm{Vol}(\overline{A})}{9}. \tag{11}$$

Since Kershner formulates the problem with closed discs whereas we formulate problem (1,2) with open discs and open sets A, we assume, for comparison purposes, that the results of Kershner still hold for $A \in \mathcal{S}$, for which we have $\mathrm{Vol}(\overline{A}) = \mathrm{Vol}(A)$. Let $r^*(m)$ be the solution to problem (1,2), viewed as a function of m. Clearly we have $r^*(m_0) \geq r^*(m_1)$ if $m_0 < m_1$. Indeed, if we have a covering of A with m_0 balls of radius $r^*(m_0)$, then we can place $m_1 - m_0$ balls of radius $r^*(m_0)$ at random positions to get a covering of A with m_1 balls of radius $r^*(m_0)$, thus $r^*(m_1)$ must be smaller or equal to $r^*(m_0)$.

Now, since we have a covering of A with m balls of radius $r^*(m)$, we must have $N(r^*(m)) \leq m$. Note that, maybe unexpectedly, the case $N(r^*(m)) < m$ may occur, for instance in the case where A is a union of rings and balls of radius $r^*(m)$ that do not overlap and are sufficiently far apart from each other. We start with the following intermediary result.

Lemma 1. *For $A \in \mathcal{S}$ we have $r^*(m) \to 0$ as $m \to \infty$, $r^*(m) = r^*(f(m))$, where $f(m) := N(r^*(m))$, and*

$$\lim_{m \to \infty} \pi r^*(f(m))^2 f(m) = \frac{2\pi\sqrt{3}\,\mathrm{Vol}(A)}{9}. \tag{12}$$

Proof. Since A is bounded, let S be the smallest square containing A and let L be the square's edge length. We may divide S into $\lfloor\sqrt{m}\rfloor^2$ smaller squares with edge length $L/\lfloor\sqrt{m}\rfloor$, where $\lfloor\sqrt{m}\rfloor$ is the largest integer smaller or equal to $\sqrt{m}$. Then we can cover each small square by a disc of radius $\sqrt{2}L/(2\lfloor\sqrt{m}\rfloor)$, and the union of these $\lfloor\sqrt{m}\rfloor^2$ discs, where $\lfloor\sqrt{m}\rfloor^2 \leq m$, clearly covers S and hence also A. Thus $r^*(m) \leq \sqrt{2}L/(2\lfloor\sqrt{m}\rfloor)$ which shows that $r^*(m) \to 0$ as $m \to \infty$.

On the one hand, since $f(m) \leq m$ and $m \mapsto r^*(m)$ is decreasing, we have $r^*(f(m)) \geq r^*(m)$. On the other hand there exists a covering of A with $f(m)$ balls of radius $r^*(m)$, thus $r^*(f(m)) \leq r^*(m)$. This proves $r^*(m) = r^*(f(m))$.

Finally, taking $r = r^*(m)$ in (11), using $r^*(m) = r^*(f(m))$ and $\mathrm{Vol}(\overline{A}) = \mathrm{Vol}(A)$ we get (12). □

This implies the following asymptotic result.

Lemma 2. *For $A \in \mathcal{S}$, the solution to problem (1,2) satisfies*

$$\liminf_{m \to \infty} r^*(m)\sqrt{m} = \left[\frac{2\,\mathrm{Vol}(A)}{3\sqrt{3}}\right]^{1/2}. \tag{13}$$

Proof. Since $N(r^*(m)) \le m$, taking $r = r^*(m)$ in (11), using $r^*(m) \to 0$ as $m \to \infty$ and $\mathrm{Vol}(\overline{A}) = \mathrm{Vol}(A)$ we get

$$\liminf_{m\to\infty} r^*(m)\sqrt{m} \ge \lim_{m\to\infty} r^*(m)\sqrt{N(r^*(m))} = \left[\frac{2\,\mathrm{Vol}(A)}{3\sqrt{3}}\right]^{1/2}. \tag{14}$$

In view of (12) we also have

$$\left[\frac{2\,\mathrm{Vol}(A)}{3\sqrt{3}}\right]^{1/2} = \lim_{m\to\infty} r^*(f(m))\sqrt{f(m)} \ge \liminf_{m\to\infty} r^*(m)\sqrt{m}.$$

This yields (13). □

The lim inf appearing in (13) instead of a simple limit is directly related to the possible case $N(r^*(m)) < m$. Such situation may in principle occur for pathological sets A since no regularity is assumed on A in the paper of Kershner [24], but we expect the condition $N(r^*(m)) = m$ to be satisfied for domains A with sufficient regularity and m sufficiently large. We show indeed in Theorem 1 a result similar to (13) for $A \in \mathcal{S}$, but with a simple limit instead of a limit inferior, and we provide asymptotic bounds for the remainder. Thus, our main result yields a more precise asymptotic expansion of $r^*(m)$ with respect to m, albeit for a smaller class of sets A. We also conclude that problem (1,2) and Kershner's problem of determining $N(r)$ are similar but not exactly equivalent.

From the methodological point of view, Kershner also uses a trapping of the set A between a subset and a supset. The main difference is that his trapping subset and supset are unions of rectangles, while we use hexagonal honeycombs. In order to deduce lower and upper bounds for the covering of A, he proves and uses the following lower and upper bounds for the minimal number of identical discs required to cover a rectangle D:

$$\frac{2\pi}{3\sqrt{3}}(\mathrm{Vol}(D) - 2\pi r^2) < \pi r^2 N(r) < \frac{2\pi}{3\sqrt{3}}(\mathrm{Vol}(D) + 2r\,\mathrm{Per}(\partial D) + 16r^2). \tag{15}$$

The main drawback of this approach is that the shapes and the amount of rectangles required to define the trapping subset and supset are unknown and seem difficult to control. This allows him to obtain the asymptotic estimate (11), but the higher-order terms of the lower and upper bounds for rectangles in (15) are lost in the process. By contrast, in our approach, the advantage of using hexagonal honeycombs for the trapping sets is that the optimal covering radius is known exactly and the shape of these honeycombs is easier to control, which allows us to obtain higher-order terms in the asymptotic expansion of $r^*(m)$.

The optimal radius for coverings of honeycombs based on regular hexagonal lattice can be obtained using the thinnest covering property of the regular hexagonal lattice arrangement in the whole plane. We use this property, as well as the fact that the trapping honeycombs converge in some sense to A as the number m of balls goes to infinity, to obtain estimates on the optimal radius $r^*(m)$ for (1,2). One technical difficulty along this way is that the honeycombs H_0 and H_1 need to be the union of exactly m regular hexagons so that the optimal radii can be compared, which requires a few adjustments. In order to prove that the upper honeycomb H_0 converges to A, we show that it is contained in a set containing A that converges to A as $m \to \infty$, and whose area can be estimated as a function of m. A similar procedure is used to obtain the convergence of H_1 towards A.

Before stating the main result of this section, we need a few notations. Introduce the hexagonal lattice

$$\mathcal{L}_r := \{kv_r + \ell w_r \mid (k,\ell) \in \mathbb{Z}^2\} \tag{16}$$

with $v_r := \frac{r}{2}(3, \sqrt{3})$ and $w_r := \frac{r}{2}(3, -\sqrt{3})$; see Figure 1.

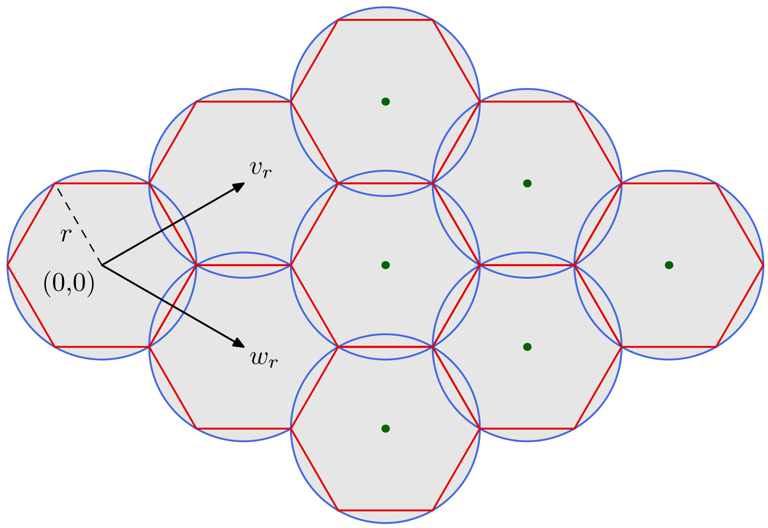

Figure 1: Example of an hexagonal lattice $\mathcal{L}_r$ as defined in (16). The picture displays elements with k and $\ell \in \{0,1,2\}$ only.

Let $A_h = \{x \in \mathbb{R}^2 \mid d(x,A) < h\}$, then we define

$$r_0(m,h) := \arg\inf\{r \in \mathbb{R} \mid |\mathcal{L}_r \cap A_h| \leq m\}, \tag{17}$$

recalling that $|\mathcal{L}_r \cap A_h|$ denotes the cardinal of $\mathcal{L}_r \cap A_h$. We will sometimes write r_0 instead of $r_0(m,h)$ for simplicity.

The plane $\mathbb{R}^2$ can be tiled by the following regular hexagons with centers at the points of the hexagonal lattice $\mathcal{L}_r$:

$$P_r(z) := \{x \in \mathbb{R}^2 \mid \|x - z\| \leq \|x - y\| \ \text{ for all } y \in \mathcal{L}_r\}.$$

For a sublattice $L \subset \mathcal{L}_r$ we define the *honeycomb*

$$H(L) := \bigcup_{z \in L} P_r(z). \tag{18}$$

The main result of this section is the following asymptotic upper and lower bounds on the optimal radius $r^*(m)$ for the minimization problem (1,2), whose proof is given in Section 3.4.

Theorem 1. *Let $A \in \mathcal{S}$. There exists $\overline{m} \in \mathbb{N}$ with $\overline{m} \geq 16\pi\bar{k}/(3\sqrt{3})$ such that, for all $m > \overline{m}$, the solution $r^*(m)$ to the minimization problem (1,2) satisfies*

$$r^*(m) = \left[\frac{2\,\mathrm{Vol}(A)}{3\sqrt{3}m}\right]^{1/2} + R(m) \tag{19}$$

with

$$\underline{R}(m) \leq R(m) \leq \overline{R}(m), \tag{20}$$

where

$$\underline{R}(m) := -\frac{2\,\mathrm{Per}(\partial A)}{3\sqrt{3}m} - \frac{8\pi\bar{k}(2\,\mathrm{Vol}(A))^{1/2}}{(3\sqrt{3}m)^{3/2}}, \quad \overline{R}(m) := \frac{2\mu_m\,\mathrm{Per}(\partial A) + 8\pi\bar{k}\mu_m^2}{\left(2\,\mathrm{Vol}(A)3\sqrt{3}m\right)^{1/2}},$$

$$\mu_m := \frac{2\,\mathrm{Per}(\partial A) + [4\,\mathrm{Per}(\partial A)^2 + 2\,\mathrm{Vol}(A)(3\sqrt{3}m - 10\pi\bar{k})]^{1/2}}{3\sqrt{3}m - 16\pi\bar{k}}. \tag{21}$$

In addition, the following asymptotic expansion holds as $m \to \infty$:

$$\overline{R}(m) = \frac{2\,\mathrm{Per}(\partial A)}{3\sqrt{3}m} + \frac{4\,\mathrm{Per}(\partial A)^2 + 16\pi\bar{k}\,\mathrm{Vol}(A)}{(2\,\mathrm{Vol}(A))^{1/2}(3\sqrt{3}m)^{3/2}} + O\left(\frac{1}{m^2}\right). \tag{22}$$

We conclude this section by comparing (19) in the particular case of a rectangle with the asymptotic bounds implied by (15). Taking $r = r^*(m)$ in (15) and assuming that $N(r^*(m)) = m$, it can be shown that (15) implies the following bounds for sufficiently large m for the problem of covering a rectangle D:

$$\underline{S}(m) < r^*(m) < \overline{S}(m),$$

where

$$\underline{S}(m) := \left(\frac{2\,\mathrm{Vol}(D)}{3\sqrt{3}m + 4\pi}\right)^{1/2} \quad \text{and} \quad \overline{S}(m) := \frac{2\,\mathrm{Per}(\partial D) + (4\,\mathrm{Per}(\partial D)^2 + 2\,\mathrm{Vol}(D)(3\sqrt{3}m - 32))^{1/2}}{(3\sqrt{3}m - 32)}.$$

Asymptotically, we have

$$\overline{S}(m) = \left[\frac{2\,\mathrm{Vol}(D)}{3\sqrt{3}m}\right]^{1/2} + \frac{2\,\mathrm{Per}(\partial D)}{3\sqrt{3}m} + O(m^{-3/2}), \tag{23}$$

$$\underline{S}(m) = \left[\frac{2\,\mathrm{Vol}(D)}{3\sqrt{3}m}\right]^{1/2} - \frac{2\pi(2\,\mathrm{Vol}(D))^{1/2}}{(3\sqrt{3}m)^{3/2}} + O(m^{-5/2}). \tag{24}$$

On the one hand, we observe that the term $2\,\mathrm{Per}(\partial D)/(3\sqrt{3}m)$ in (23) is the same as the first-order term in (22), and the next term in (23) is of order $m^{-3/2}$ as in (22). On the other hand, the second-order term in (24) is of order $m^{-3/2}$, whereas the second-order term in the lower bound of (19) is of order m^{-1}. This better rate may be explained by the fact that the lower bound in (15) is obtained using a technique based on Voronoi cells which is specific to rectangles; note that this lower bound was also improved by Verblunksy [37] for the particular case of squares. We also mention that asymptotic bounds for $N(r)$ have also been obtained in the case of spheres [38].

Thus, we gather from this comparison that Theorem 1 provides a refined asymptotic estimate for the optimal radius $r^*(m)$ with respect to m, compared with (13), that is valid for the general class of bounded set $A \in \mathcal{S}$. The upper bound in Theorem 1 is similar to the upper bound obtained by Kershner in [24] for rectangles, whereas the lower bound in Theorem 1 is less sharp than the lower bound obtained for rectangles. An interesting direction for research would be to determine whether the bounds (20) are sharp or not for $A \in \mathcal{S}$ by studying asymptotic expansions for specific shapes.

3.1 Upper honeycomb

In this section and in the rest of Section 3 we always assume that $A \in \mathcal{S}$. As described above, the first step is to build an upper honeycomb $H(L_0)$ that contains A, is included in $\overline{A_{h+r}}$ for some appropriate values of h and r, and is the union of exactly m polygons, where L_0 is an appropriate subset of $\mathcal{L}_r$. The natural candidates for $H(L_0)$ are the honeycombs $H(\mathcal{L}_{r_0(m,h)} \cap A_h)$ and $H(\mathcal{L}_{r_0(m,h)} \cap \overline{A_h})$. However, Lemma 3 below implies that $H(\mathcal{L}_{r_0(m,h)} \cap \overline{A_h})$ always contains at least $m+1$ polygons, while $H(\mathcal{L}_{r_0(m,h)} \cap A_h)$ contains at most m polygons. Thus, one needs to choose $H(L_0)$ as the honeycomb $H(\mathcal{L}_{r_0(m,h)} \cap \widehat{A})$, where $\widehat{A}$ is some appropriate set satisfying $A_h \subset \widehat{A} \subset \overline{A_h}$.

Lemma 3. *We have* $|\mathcal{L}_{r_0(m,h)} \cap A_h| \leq m$ *and* $|\mathcal{L}_{r_0(m,h)} \cap \overline{A_h}| \geq m+1$.

Proof. Clearly we have $r_0(m,h) > 0$. Let $\{r_n\}_{n\in\mathbb{N}}$ be a sequence satisfying $|\mathcal{L}_{r_n} \cap A_h| \leq m$ and $r_n \to r_0(m,h)$ as $n \to +\infty$. Let $\mathcal{Z}^- \subset \mathbb{Z}^2$ be such that

$$\mathcal{L}_{r_0(m,h)} \cap A_h = \{k\, v_{r_0(m,h)} + \ell\, w_{r_0(m,h)} \mid (k,\ell) \in \mathcal{Z}^-\}.$$

Since A_h is open, there exists $n_0 \in \mathbb{N}$ such that, for all $n \geq n_0$,

$$\mathcal{L}_{r_n} \cap A_h = \{k\, v_{r_n} + \ell\, w_{r_n} \mid (k,\ell) \in \mathcal{Z}^-\}$$

and $|\mathcal{L}_{r_n} \cap A_h| = |\mathcal{L}_{r_0(m,h)} \cap A_h| = |\mathcal{Z}^-|$. Since $|\mathcal{L}_{r_n} \cap A_h| \leq m$ for all n, we get $|\mathcal{L}_{r_0(m,h)} \cap A_h| \leq m$, which proves the first part of the lemma.

Now let $\varepsilon_n > 0$ be a sequence converging to 0, then we have $|\mathcal{L}_{r_0(m,h)-\varepsilon_n} \cap A_h| \geq m+1$ for all $n \in \mathbb{N}$, otherwise there would be a contradiction with (17). We also have

$$\lim_{n\to\infty} \mathcal{L}_{r_0(m,h)-\varepsilon_n} \cap A_h \subset \mathcal{L}_{r_0(m,h)} \cap \overline{A_h},$$

thus

$$m+1 \leq \lim_{n\to\infty} |\mathcal{L}_{r_0(m,h)-\varepsilon_n} \cap A_h| \leq |\mathcal{L}_{r_0(m,h)} \cap \overline{A_h}|$$

and this proves the second part of the lemma. $\square$

In view of the results of Lemma 3 and since we need a set $L_0 \subset \mathcal{L}_r$ satisfying $|L_0| = m$, the strategy is to complete $\mathcal{L}_{r_0(m,h)} \cap A_h$ with points from the boundary of A_h. Let $\mathcal{Z}^+ \subset \mathbb{Z}^2$ be such that

$$\mathcal{L}_{r_0(m,h)} \cap \overline{A_h} = \{k\, v_{r_0(m,h)} + \ell\, w_{r_0(m,h)} \mid (k,\ell) \in \mathcal{Z}^+\}.$$

In view of Lemma 3 we have $|\mathcal{Z}^-| \leq m$ and $|\mathcal{Z}^+| \geq m+1$. There exists $\mathcal{Z} \subset \mathbb{Z}^2$ such that $\mathcal{Z}^- \subset \mathcal{Z} \subset \mathcal{Z}^+$ and $|\mathcal{Z}| = m$. We can now introduce the sublattice

$$L_0(m,h) := \{k\, v_{r_0(m,h)} + \ell\, w_{r_0(m,h)} \mid (k,\ell) \in \mathcal{Z}\}. \tag{25}$$

Thus we get

$$\mathcal{L}_{r_0(m,h)} \cap A_h \subset L_0(m,h) \subset \mathcal{L}_{r_0(m,h)} \cap \overline{A_h} \tag{26}$$

and the sublattice $L_0(m,h)$ satisfies indeed the desired property $|L_0(m,h)| = m$. Further, the role of the upper honeycomb H_0 will be played by $H(L_0(m,h))$ for specific values of h.

Now that we have found our candidate $H(L_0(m,h))$ for the upper honeycomb, we need to prove the inclusions $A \subset H(L_0(m,h)) \subset \overline{A_{h+r_0(m,h)}}$ which will be key to obtain estimates for the optimal covering radius $r^*(m)$ of A. We start by proving general inclusions for the honeycombs $H(\mathcal{L}_r \cap \overline{A_h})$ and $H(\mathcal{L}_r \cap A_h)$.

Lemma 4. *We have $H(\mathcal{L}_r \cap \overline{A_h}) \subset \overline{A_{h+r}}$ for all $r > 0$ and $h > 0$.*

Proof. Let $x \in H(\mathcal{L}_r \cap \overline{A_h})$, then $d(x, \mathcal{L}_r \cap \overline{A_h}) \leq r$ by (18) and there exists $z \in \mathcal{L}_r \cap \overline{A_h}$ such that $d(x, z) \leq r$. Since $z \in \overline{A_h}$, $d(z, A) \leq h$ by definition of A_h. Thus $d(x, A) \leq d(x, z) + d(z, A) \leq r + h$. This shows that $x \in \overline{A_{h+r}}$ and $H(\mathcal{L}_r \cap \overline{A_h}) \subset \overline{A_{h+r}}$. □

Lemma 5. *If $h \geq r$ then $A \subset H(\mathcal{L}_r \cap A_h)$.*

Proof. It can be checked that the maximal radius of $P_r(z)$ is r. Let $x \in A$, since $\cup_{z \in \mathcal{L}_r} P_r(z)$ is a tiling of $\mathbb{R}^2$, there exists $z \in \mathcal{L}_r$ such that $x \in P_r(z)$ and hence $\|x - z\| \leq r \leq h$, which implies $z \in \mathcal{L}_r \cap \overline{A_h}$. If $z \in \mathcal{L}_r \cap \partial A_h$, then $d(z, A) = h$. Thus $\|x - z\| \geq h$ which would imply $x \in \partial A$, a contradiction with $x \in A$. Hence $z \in \mathcal{L}_r \cap A_h$ and then $d(x, \mathcal{L}_r \cap A_h) \leq r$, which implies that $A \subset H(\mathcal{L}_r \cap A_h)$ since the maximal radius of the hexagon $P_r(z)$ in $H(\mathcal{L}_r \cap A_h)$ is r. □

Since $r_0(m, h)$ depends on h, it is not clear if the condition $h \geq r$ of Lemma 5 can be satisfied for $r = r_0(m, h)$. The purpose of the following lemma is to show that this condition can actually be satisfied for m sufficiently large.

Lemma 6. *We have the following expansion as $m \to \infty$:*

$$0 < \mu_m = \left(\frac{2 \operatorname{Vol}(A)}{3\sqrt{3}m} \right)^{1/2} + \frac{2 \operatorname{Per}(\partial A)}{3\sqrt{3}m} + O\left(\frac{1}{m^{3/2}} \right), \tag{27}$$

where μ_m is defined in (21). In addition, let $\{h_m\}_{m \geq 0}$ satisfying $h_m \to 0$ as $m \to +\infty$ and $h_m \geq \mu_m$ for all $m \geq 16\pi\bar{k}/(3\sqrt{3})$, then there exists $m_1 \geq 16\pi\bar{k}/(3\sqrt{3})$ such that $h_m \geq r_0(m, h_m)$ for all $m \geq m_1$.

Proof. Let $\{h_m\}_{m \geq 0}$ satisfying $h_m \to 0$ as $m \to +\infty$. Using Lemma 4 and (26) we get

$$H(L_0(m, h_m)) \subset H(\mathcal{L}_{r_0(m, h_m)} \cap \overline{A_{h_m}}) \subset \overline{A_{h_m + r_0(m, h_m)}},$$

hence $\operatorname{Vol}(H(L_0(m, h_m))) \leq \operatorname{Vol}(A_{h_m + r_0(m, h_m)})$. By definition (25) of $L_0(m, h)$, and since the area of a regular polygon of maximal radius $r_0(m, h_m)$ is $\frac{3\sqrt{3}}{2} r_0(m, h_m)$, we get

$$\frac{3\sqrt{3}}{2} r_0(m, h_m)^2 m \leq \operatorname{Vol}(A_{h_m + r_0(m, h_m)}). \tag{28}$$

Since A is bounded, there exists an open disc $B(\hat{x}, \hat{r})$ such that $A \subset B(\hat{x}, \hat{r})$ with minimal radius $\hat{r}$. We also have $A_h \subset B(\hat{x}, \hat{r} + h)$ and $\operatorname{Vol}(A_h) \leq \pi(\hat{r} + h)^2$. Using (28) this yields

$$\frac{3\sqrt{3}}{2} r_0(m, h_m)^2 m \leq \operatorname{Vol}(A_{h_m + r_0(m, h_m)}) \leq \pi(\hat{r} + h_m + r_0(m, h_m))^2. \tag{29}$$

Since $h_m \to 0$, this proves that $r_0(m, h_m) \to 0$ as $m \to +\infty$.

Let $\Gamma_k^h := \{x \in \mathbb{R}^2 \mid d(x, \Gamma_k) < h\} \cap A^c$, where $\{x \in \mathbb{R}^2 \mid d(x, \Gamma_k) < h\}$ is the so-called *tubular neighborhood* of Γ_k, and $\Gamma_k \subset \partial A$ is one of the arcs in the decomposition (10). We can show that

$$A_h \subset \left(A \cup \left(\bigcup_{k=1}^{\bar{k}} \Gamma_k^h \right) \right), \tag{30}$$

see [9, Theorem 4.1].

Let $\mathcal{V}_k$ be the set of endpoints of the arc Γ_k, then $\mathcal{V}_k$ is included in the set of vertices of ∂A and contains at most two vertices. For sufficiently small h, Γ_k^h satisfies

$$\Gamma_k^h \subset \{x + \nu(x)\mu \mid x \in \overline{\Gamma_k}, 0 \leq \mu < h\} \cup \bigcup_{z \in \mathcal{V}_k} \mathbb{B}(z),$$

where $\mathbb{B}(z)$ is an open ball with center z and radius h, and $\nu(x)$ is a normal vector to $\overline{\Gamma_k}$ at x. Using the results of [22, Chapter 1], there exists $\bar{h}_k > 0$ such that

$$\mathrm{Vol}(\{x + \nu(x)\mu \mid x \in \overline{\Gamma_k}, 0 \leq \mu < h\}) = h\,\mathrm{Per}(\Gamma_k) \quad \forall h \text{ such that } 0 < h \leq \bar{h}_k.$$

Since $\mathcal{V}_k$ contains at most two vertices, we obtain $\mathrm{Vol}(\Gamma_k^h) \leq h\,\mathrm{Per}(\Gamma_k) + 2\pi h^2$ for all h such that $0 < h \leq \bar{h}_k$. As there is a finite number of arcs Γ_k, there exists $\bar{h} > 0$ such that $\sum_{k=1}^{\bar{k}} \mathrm{Vol}(\Gamma_k^h) \leq h\,\mathrm{Per}(\partial A) + 2\pi\bar{k}h^2$ for all h such that $0 < h \leq \bar{h}$.

This yields for $0 < h \leq \bar{h}$, using (30),

$$\mathrm{Vol}(A_h) \leq \mathrm{Vol}(A) + \sum_{k=1}^{\bar{k}} [h\,\mathrm{Per}(\Gamma_k) + 2\pi h^2] = \mathrm{Vol}(A) + h\,\mathrm{Per}(\partial A) + 2\pi\bar{k}h^2. \tag{31}$$

Using $h_m \to 0$ and $r_0(m, h_m) \to 0$ as $m \to \infty$, there exists $m_1 \in \mathbb{N}$ such that $h_m + r_0(m, h_m) \leq \bar{h}$ for all $m \geq m_1$. This yields, using (28) and (31),

$$\frac{3\sqrt{3}}{2} r_0(m, h_m)^2 m \leq \mathrm{Vol}(A) + (h_m + r_0(m, h_m))\,\mathrm{Per}(\partial A) + 2\pi\bar{k}(h_m + r_0(m, h_m))^2. \tag{32}$$

Then, writing (32) in the form $\alpha_1 r_0^2 + \alpha_2 r_0 + \alpha_3 \leq 0$ and studying the variations of the polynomial $\alpha_1 r_0^2 + \alpha_2 r_0 + \alpha_3$ we obtain that (32) and $r_0 > 0$ are equivalent to

$$0 < r_0(m, h_m) \leq \frac{\mathrm{Per}(\partial A) + 4\pi\bar{k}h_m + \sqrt{\Delta_m}}{C_m}, \tag{33}$$

with $C_m := 3\sqrt{3}m - 4\pi\bar{k}$ and $\Delta_m := (\mathrm{Per}(\partial A) + 4\pi\bar{k}h_m)^2 + 2C_m\left(\mathrm{Vol}(A) + h_m\,\mathrm{Per}(\partial A) + 2\pi\bar{k}h_m^2\right)$, where we have assumed that $C_m > 0$, so that $\Delta_m > 0$.

Next, we establish a sufficient condition for

$$\frac{\mathrm{Per}(\partial A) + 4\pi\bar{k}h_m + \sqrt{\Delta_m}}{C_m} \leq h_m \tag{34}$$

to hold. Inequality (34) may be written as follows:

$$0 \leq h_m^2[C_m(C_m - 12\pi\bar{k})] + h_m[-4\,\mathrm{Per}(\partial A)C_m] - 2C_m\,\mathrm{Vol}(A).$$

Assuming that $C_m - 12\pi\bar{k} > 0$, which is equivalent to $m > \frac{16\pi\bar{k}}{3\sqrt{3}}$, the two roots of this polynomial in h_m are

$$\frac{4\,\mathrm{Per}(\partial A)C_m \pm [4C_m^2(4\,\mathrm{Per}(\partial A)^2 + 2\,\mathrm{Vol}(A)(C_m - 12\pi\bar{k}))]^{1/2}}{2C_m(C_m - 12\pi\bar{k})}$$

Since $C_m - 12\pi\bar{k} > 0$, the smallest of these two roots is negative and the largest is positive. Thus (34) is satisfied if

$$h_m \geq \mu_m := \frac{2\,\mathrm{Per}(\partial A) + [4\,\mathrm{Per}(\partial A)^2 + 2\,\mathrm{Vol}(A)(C_m - 12\pi\bar{k})]^{1/2}}{C_m - 12\pi\bar{k}}.$$

Now we provide an asymptotic expansion of μ_m. We first write $\mu_m = \mu_m^{(1)}/\mu_m^{(2)}$, where

$$\mu_m^{(1)} := \frac{2\,\mathrm{Per}(\partial A) + [4\,\mathrm{Per}(\partial A)^2 + 2\,\mathrm{Vol}(A)(C_m - 12\pi\bar{k})]^{1/2}}{m} \quad \text{and} \quad \mu_m^{(2)} := \frac{C_m - 12\pi\bar{k}}{m}.$$

This yields

$$\begin{aligned}
\mu_m^{(1)} &= \frac{2\,\mathrm{Per}(\partial A)}{m} + \left(\frac{6\sqrt{3}\,\mathrm{Vol}(A)}{m}\right)^{1/2} \left(1 + \frac{2\,\mathrm{Per}(\partial A)^2}{3\sqrt{3}\,\mathrm{Vol}(A)m} - \frac{16\pi\bar{k}}{3\sqrt{3}m}\right)^{1/2}, \\
\mu_m^{(2)} &= 3\sqrt{3}\left(1 - \frac{16\pi\bar{k}}{3\sqrt{3}m}\right),
\end{aligned}$$

and then

$$\begin{aligned}
\mu_m^{(1)} &= \left(\frac{6\sqrt{3}\,\mathrm{Vol}(A)}{m}\right)^{1/2} + \frac{2\,\mathrm{Per}(\partial A)}{m} + O\left(\frac{1}{m^{3/2}}\right), \\
\frac{1}{\mu_m^{(2)}} &= \frac{1}{3\sqrt{3}} + O\left(\frac{1}{m}\right).
\end{aligned}$$

This yields

$$\mu_m = \frac{\mu_m^{(1)}}{\mu_m^{(2)}} = \left(\frac{2\,\mathrm{Vol}(A)}{3\sqrt{3}m}\right)^{1/2} + \frac{2\,\mathrm{Per}(\partial A)}{3\sqrt{3}m} + O\left(\frac{1}{m^{3/2}}\right),$$

which proves the result. □

Combining Lemma 5 and Lemma 6 shows that for any sequence $\{h_m\}_{m\geq 0}$ converging to 0 and satisfying $h_m \geq \mu_m$, we have $A \subset H(\mathcal{L}_{r_0(m,h_m)} \cap A_{h_m})$ for all $m \geq m_1 \geq 16\pi\bar{k}/(3\sqrt{3})$. We are now ready to state the asymptotic expansion of $r_0(m, \mu_m)$ with respect to m.

Theorem 2. *There exists $m_0 \in \mathbb{N}$ with $m_0 \geq 16\pi\bar{k}/(3\sqrt{3})$ such that, for all $m \geq m_0$, the following asymptotic expansion holds:*

$$r_0(m, \mu_m) = \left[\frac{2\,\mathrm{Vol}(A)}{3\sqrt{3}m}\right]^{1/2} + R_0(m)$$

with

$$0 \leq R_0(m) \leq \frac{2\mu_m\,\mathrm{Per}(\partial A) + 8\pi\bar{k}\mu_m^2}{\left(2\,\mathrm{Vol}(A)3\sqrt{3}m\right)^{1/2}} = \frac{2\,\mathrm{Per}(\partial A)}{3\sqrt{3}m} + \frac{4\,\mathrm{Per}(\partial A)^2 + 16\pi\bar{k}\,\mathrm{Vol}(A)}{(2\,\mathrm{Vol}(A))^{1/2}(3\sqrt{3}m)^{3/2}} + O\left(\frac{1}{m^2}\right).$$

Proof. Using (26) and Lemmas 4, 5 and 6, we get

$$A \subset H(\mathcal{L}_{r_0(m,\mu_m)} \cap A_{\mu_m}) \subset H(L_0(m,\mu_m)) \subset H(\mathcal{L}_{r_0(m,\mu_m)} \cap \overline{A_{\mu_m}}) \subset \overline{A_{\mu_m+r_0(m,\mu_m)}}$$

for $m \geq m_1 \geq 16\pi\bar{k}/(3\sqrt{3})$. Thus

$$\mathrm{Vol}(A) \leq \mathrm{Vol}(H(L_0(m,\mu_m))) \leq \mathrm{Vol}(A_{\mu_m+r_0(m,\mu_m)}). \tag{35}$$

Using (28), (31), (35), and $\mu_m + r_0(m,\mu_m) \to 0$ as $m \to +\infty$ yields

$$0 \leq \frac{3\sqrt{3}}{2} r_0(m,\mu_m)^2 m - \mathrm{Vol}(A) \leq (\mu_m + r_0(m,\mu_m))\,\mathrm{Per}(\partial A) + 2\pi\bar{k}(\mu_m + r_0(m,\mu_m))^2$$

and

$$0 \leq r_0(m,\mu_m)^2 - \frac{2\,\mathrm{Vol}(A)}{3\sqrt{3}m} \leq \frac{2(\mu_m + r_0(m,\mu_m))\,\mathrm{Per}(\partial A) + 4\pi\bar{k}(\mu_m + r_0(m,\mu_m))^2}{3\sqrt{3}m}.$$

Then

$$0 \leq r_0(m,\mu_m) - \left(\frac{2\,\mathrm{Vol}(A)}{3\sqrt{3}m}\right)^{1/2} \leq \mathcal{R}(m,\mu_m) \tag{36}$$

with

$$\mathcal{R}(m,\mu_m) := \frac{2(\mu_m + r_0(m,\mu_m))\,\mathrm{Per}(\partial A) + 4\pi\bar{k}(\mu_m + r_0(m,\mu_m))^2}{3\sqrt{3}m\left(r_0(m,\mu_m) + \left(\frac{2\,\mathrm{Vol}(A)}{3\sqrt{3}m}\right)^{1/2}\right)}.$$

Using Lemma 6 and (36) we have $\left(\frac{2\,\mathrm{Vol}(A)}{3\sqrt{3}m}\right)^{1/2} < r_0(m,\mu_m) \leq \mu_m$, this yields

$$\mathcal{R}(m,\mu_m) \leq \frac{4\mu_m\,\mathrm{Per}(\partial A) + 16\pi\bar{k}\mu_m^2}{6\sqrt{3}m\left(\frac{2\,\mathrm{Vol}(A)}{3\sqrt{3}m}\right)^{1/2}} = \frac{2\mu_m\,\mathrm{Per}(\partial A) + 8\pi\bar{k}\mu_m^2}{\left(2\,\mathrm{Vol}(A)3\sqrt{3}m\right)^{1/2}}.$$

Then, using (27) we get, as $m \to \infty$,

$$\frac{2\mu_m\,\mathrm{Per}(\partial A) + 8\pi\bar{k}\mu_m^2}{\left(2\,\mathrm{Vol}(A)3\sqrt{3}m\right)^{1/2}} = \frac{2\,\mathrm{Per}(\partial A)}{3\sqrt{3}m} + \frac{4\,\mathrm{Per}(\partial A)^2 + 16\pi\bar{k}\,\mathrm{Vol}(A)}{(2\,\mathrm{Vol}(A))^{1/2}(3\sqrt{3}m)^{3/2}} + O\left(\frac{1}{m^2}\right).$$

This proves the result. □

3.2 Lower honeycomb

In Section 3.1 we have built an upper honeycomb $H(L_0(m,\mu_m))$ that contains A, is included in $\overline{A_{\mu_m+r_0(m,\mu_m)}}$, and is the union of exactly m polygons. Following a similar procedure, we now build a lower honeycomb $H(L_1)$, where L_1 is a subset of $\mathcal{L}_r$, that is included in $\overline{A}$ and contains A_{-h-r} for some appropriate values of h and r, where

$$A_{-h} := \{x \in \mathbb{R}^2 \mid d(x, A^c) > h\}$$

for $h > 0$. We also introduce

$$r_1(m,h) := \arg\inf\{r \in \mathbb{R} \mid |\mathcal{L}_r \cap A_{-h}| \leq m\}, \tag{37}$$

where $|\mathcal{L}_r \cap A_{-h}|$ denotes the cardinal of $\mathcal{L}_r \cap A_{-h}$. We will sometimes write r_1 instead of $r_1(m,h)$ for simplicity. We omit the proof of the following result, which is similar to the proof of Lemma 3.

Lemma 7. *We have* $|\mathcal{L}_{r_1(m,h)} \cap A_{-h}| \leq m$ *and* $|\mathcal{L}_{r_1(m,h)} \cap \overline{A_{-h}}| \geq m+1$.

Since we need a sublattice L_1 satisfying $|L_1| = m$, neither $\mathcal{L}_{r_1(m,h)} \cap A_{-h}$ nor $\mathcal{L}_{r_1(m,h)} \cap \overline{A_{-h}}$ can play the role of L_1 in view of Lemma 7, but we may complete $\mathcal{L}_{r_1(m,h)} \cap A_{-h}$ with a few points from the boundary of A_{-h} to obtain L_1. Proceeding as in the definition of $L_0(m,h)$ in Section 3.1 we obtain the existence of a sublattice $L_1(m,h)$ satisfying

$$\mathcal{L}_{r_1(m,h)} \cap A_{-h} \subset L_1(m,h) \subset \mathcal{L}_{r_1(m,h)} \cap \overline{A_{-h}} \tag{38}$$

and $|L_1(m,h)| = m$. Further, the role of the lower honeycomb H_1 will be played by $H(L_1(m,h))$ for specific values of h.

Now we need to prove the inclusions $A_{-h-r_1(m,h)} \subset H(L_1(m,h)) \subset \overline{A}$ which will be key to obtain estimates for the optimal covering radius $r^*(m)$. We start by proving general inclusions for the honeycombs $H(\mathcal{L}_r \cap \overline{A_{-h}})$ and $H(\mathcal{L}_r \cap A_{-h})$.

Lemma 8. *We have* $H(\mathcal{L}_r \cap \overline{A_{-h}}) \subset \overline{A}$ *if* $h \geq r$ *and* $H(\mathcal{L}_r \cap \overline{A_{-h}}) \subset \overline{A_{-h+r}}$ *if* $h < r$.

Proof. Let $x \in H(\mathcal{L}_r \cap \overline{A_{-h}})$, then $d(x, \mathcal{L}_r \cap \overline{A_{-h}}) \leq r$ and there exists $y \in \mathcal{L}_r \cap \overline{A_{-h}}$ such that $\|x-y\| \leq r$. Let $z \in \overline{A}^c$, then $\|y-z\| \geq h$ since $y \in \overline{A_{-h}}$. If $\|y-z\| = h$, then $z \in \partial(A^c) = \overline{A^c} \cap \overline{A}$ but this would contradict $z \in \overline{A}^c$, thus we must have $\|y-z\| > h$. Then, using $\|z-y\| \leq \|z-x\| + \|x-y\|$ we get $\|z-x\| \geq \|z-y\| - \|x-y\| > h - r \geq 0$ if $h \geq r$. Thus $\|x-z\| > 0$ for all $z \in \overline{A}^c$ if $h \geq r$, which proves $H(\mathcal{L}_r \cap \overline{A_{-h}}) \subset \overline{A}$.

In the case $h < r$, if $\|x-y\| \leq h$, then $x \in \overline{A}$ since $y \in \overline{A_{-h}}$, and consequently $x \in \overline{A_{-h+r}}$. Now if $\|x-y\| > h$, let z be the point on the segment with extremities x and y and such that $\|z-y\| = h$, then we have $\|x-z\| = \|x-y\| - \|y-z\| = \|x-y\| - h \leq r-h$. Since $\|z-y\| = h$ and $y \in \overline{A_{-h}}$, we have $z \in \overline{A}$. Thus $d(x, A) \leq \|x-z\| \leq r-h$, and consequently $x \in \overline{A_{-h+r}}$. This proves that $H(\mathcal{L}_r \cap \overline{A_{-h}}) \subset \overline{A_{-h+r}}$ if $h < r$. □

Lemma 9. *We have* $A_{-h-r} \subset H(\mathcal{L}_r \cap A_{-h})$ *for all* $r > 0$.

Proof. If $x \in A_{-h-r}$ then $d(x, A^c) > h+r$. Since $\cup_{z \in \mathcal{L}_r} P_r(z)$ is a tiling of $\mathbb{R}^2$, there exists $z \in \mathcal{L}_r$ such that $x \in P_r(z)$ and hence $\|x-z\| \leq r$. Let $y \in A^c$, then $\|x-y\| \geq d(x, A^c) > h+r$. Then $h + r < \|x-y\| \leq \|x-z\| + \|z-y\| \leq r + \|z-y\|$. Thus $\|z-y\| > h$ for all $y \in A^c$, hence $d(z, A^c) > h$. Thus $z \in A_{-h}$ and $z \in \mathcal{L}_r \cap A_{-h}$. Since $\|x-z\| \leq r$ we get $x \in H(\mathcal{L}_r \cap A_{-h})$. □

In order to prove the lower bound for $r^*(m)$, we will need the inclusion $H(\mathcal{L}_{r_1(m,h_m)} \cap \overline{A_{-h_m}}) \subset \overline{A}$ from Lemma 8, for some appropriate sequence $h_m \to 0$, which requires $h_m \geq r_1(m,h)$. Since $r_1(m,h_m)$ depends on h_m, it is not clear if this condition can be satisfied. The purpose of the following lemma is to show that it can actually be satisfied for sufficiently large m.

Lemma 10. *Let* $\{h_m\}_{m \geq 0}$ *satisfying* $h_m \to 0$ *as* $m \to +\infty$ *and*

$$h_m \geq \left(\frac{2\,\mathrm{Vol}(A)}{3\sqrt{3}m} \right)^{1/2}$$

for all $m \geq \frac{4\pi\bar{k}}{3\sqrt{3}}$. *Then there exists* $m_1 \geq \frac{4\pi\bar{k}}{3\sqrt{3}}$ *such that we have* $h_m \geq r_1(m,h_m)$ *for all* $m \geq m_1$.

Proof. Let $\{h_m\}_{m\geq 0}$ satisfying $h_m \to 0$ as $m \to +\infty$, using Lemma 8 and (38) we get

$$H(L_1(m,h_m)) \subset H(\mathcal{L}_{r_1(m,h_m)} \cap \overline{A_{-h_m}}) \subset \overline{A} \text{ if } r_1(m,h_m) \leq h_m$$

or

$$H(L_1(m,h_m)) \subset H(\mathcal{L}_{r_1(m,h_m)} \cap \overline{A_{-h_m}}) \subset \overline{A_{-h_m+r_1(m,h_m)}} \text{ if } r_1(m,h_m) > h_m.$$

Thus $\mathrm{Vol}(H(L_1(m,h_m))) \leq \mathrm{Vol}(A_{-h_m+r_1(m,h_m)})$ if $r_1(m,h_m) > h_m$ or $\mathrm{Vol}(H(L_1(m,h_m))) \leq \mathrm{Vol}(A)$ if $r_1(m,h_m) \leq h_m$.

Considering the definition of the honeycomb $H(L_1(m,h_m))$, if $r_1(m,h_m) \leq h_m$ we get

$$\frac{3\sqrt{3}}{2} r_1(m,h_m)^2 m \leq \mathrm{Vol}(A) \tag{39}$$

and then

$$r_1(m,h_m) \leq \left(\frac{2\,\mathrm{Vol}(A)}{3\sqrt{3}m}\right)^{1/2}.$$

If $r_1(m,h_m) > h_m$ we get

$$\frac{3\sqrt{3}}{2} r_1(m,h_m)^2 m \leq \mathrm{Vol}(A_{-h_m+r_1(m,h_m)}). \tag{40}$$

Since A is bounded, there exists an open disc $B(\hat{x},\hat{r})$ such that $A \subset B(\hat{x},\hat{r})$ with minimal radius $\hat{r}$. We also have $A_h \subset B(\hat{x},\hat{r}+h)$ and $\mathrm{Vol}(A_h) \leq \pi(\hat{r}+h)^2$ for any $h > 0$.

Using (39) and (40) this yields

$$\begin{aligned}
&\frac{3\sqrt{3}}{2} r_1(m,h_m)^2 m \leq \mathrm{Vol}(A), \quad \text{if } r_1(m,h_m) \leq h_m,\\
&\frac{3\sqrt{3}}{2} r_1(m,h_m)^2 m \leq \mathrm{Vol}(A_{-h_m+r_1(m,h_m)}) \leq \pi(\hat{r} - h_m + r_1(m,h_m))^2, \quad \text{if } r_1(m,h_m) > h_m.
\end{aligned}$$

Since $h_m \to 0$, this proves that $r_1(m,h_m) \to 0$ as $m \to +\infty$.

Using (31) and the fact that $-h_m + r_1(m,h_m) \to 0$, there exists $m_1 \in \mathbb{N}$ such that the following inequality holds for all $m \geq m_1$ such that $r_1(m,h_m) > h_m$:

$$\frac{3\sqrt{3}}{2} r_1(m,h_m)^2 m \leq \mathrm{Vol}(A) + (-h_m + r_1(m,h_m))\,\mathrm{Per}(\partial A) + 2\pi\bar{k}(-h_m + r_1(m,h_m))^2. \tag{41}$$

Further, suppose that $m \geq m_1$. Writing (41) in the form $\alpha_1 r_1^2 + \alpha_2 r_1 + \alpha_3 \leq 0$, and studying the variations of the polynomial $\alpha_1 r_1^2 + \alpha_2 r_1 + \alpha_3$ we obtain that (41) and $h_m < r_1(m,h_m)$ is equivalent to

$$h_m < r_1(m,h_m) \leq \frac{\mathrm{Per}(\partial A) - 4\pi\bar{k}h_m + \sqrt{\Delta_m}}{C_m}, \tag{42}$$

with $C_m := 3\sqrt{3}m - 4\pi\bar{k}$ and $\Delta_m := (\mathrm{Per}(\partial A) - 4\pi\bar{k}h_m)^2 + 2C_m\left(\mathrm{Vol}(A) - h_m\,\mathrm{Per}(\partial A) + 2\pi\bar{k}h_m^2\right)$, where we have assumed that $C_m > 0$ so that $\Delta_m > 0$.

Then, (42) implies that an inequality of the form $\beta_1 h_m^2 + \beta_2 h_m + \beta_3 < 0$ should hold. Studying the variations of the polynomial $\beta_1 h_m^2 + \beta_2 h_m + \beta_3$ we obtain that

$$0 < h_m < \left(\frac{2\,\mathrm{Vol}(A)}{3\sqrt{3}m}\right)^{1/2} \tag{43}$$

should also hold. Consequently, if $h_m \geq (2\operatorname{Vol}(A)/3\sqrt{3}m)^{1/2}$ and $C_m > 0$ hold for all $m \geq m_1$, then we must have $0 < r_1(m, h_m) \leq h_m$ for all $m \geq m_1$, otherwise (43) would have to hold for some $m \geq m_1$. This proves the result. $\square$

Theorem 3. *There exists $m_1 \in \mathbb{N}$ with $m_1 \geq \frac{4\pi\bar{k}}{3\sqrt{3}}$ such that, for all $m \geq m_1$, the following asymptotic expansion holds:*

$$r_1(m, \eta_m) = \left[\frac{2\operatorname{Vol}(A)}{3\sqrt{3}m}\right]^{1/2} + R_1(m),$$

with $\eta_m := (2\operatorname{Vol}(A)/3\sqrt{3}m)^{1/2}$ and

$$-\frac{2\operatorname{Per}(\partial A)}{3\sqrt{3}m} - \frac{8\pi\bar{k}(2\operatorname{Vol}(A))^{1/2}}{(3\sqrt{3}m)^{3/2}} \leq R_1(m) \leq 0.$$

Proof. The proof is similar to the proof of Theorem 2 so we only explain the main differences here.

Using (38) and Lemmas 8, 9 and 10 we have

$$A_{-\eta_m - r_1(m,\eta_m)} \subset H(\mathcal{L}_{r_1(m,\eta_m)} \cap A_{-\eta_m}) \subset H(L_1(m, \eta_m)) \subset H(\mathcal{L}_{r_1(m,\eta_m)} \cap \overline{A_{-\eta_m}}) \subset \overline{A}$$

for $m \geq m_1$. Thus

$$\operatorname{Vol}(A_{-\eta_m - r_1(m,\eta_m)}) \leq \operatorname{Vol}(H(L_1(m, \eta_m))) \leq \operatorname{Vol}(A). \tag{44}$$

Let $\Gamma_k^h := \{x \in \mathbb{R}^2 \mid d(x, \Gamma_k) < h\} \cap A$ where $\Gamma_k \subset \partial A$ is one of the arcs in the decomposition (10). We show that

$$A \setminus \left(\bigcup_{k=1}^{\bar{k}} \overline{\Gamma_k^h}\right) \subset A_{-h}. \tag{45}$$

Indeed, let $x \in A \setminus \left(\bigcup_{k=1}^{\bar{k}} \overline{\Gamma_k^h}\right)$ and suppose that $d(x, A^c) \leq h$, then $d(x, \partial A) \leq h$ and $d(x, \Gamma_k) \leq h$ for some $k \in \{1, \ldots, \bar{k}\}$, which implies $x \in \overline{\Gamma_k^h}$, a contradiction.

In a similar way as in the proof of Lemma 6, we can prove that there exists $\bar{h} > 0$ such that $\sum_{k=1}^{\bar{k}} \operatorname{Vol}(\Gamma_k^h) \leq h \operatorname{Per}(\partial A) + 2\pi\bar{k}h^2$ for all h such that $0 < h \leq \bar{h}$. Then, for sufficiently small h we get

$$\operatorname{Vol}\left(A \setminus \left(\bigcup_{k=1}^{\bar{k}} \overline{\Gamma_k^h}\right)\right) \geq \operatorname{Vol}(A) - \sum_{k=1}^{\bar{k}} \operatorname{Vol}(\Gamma_k^h) \geq \operatorname{Vol}(A) - h\operatorname{Per}(\partial A) - 2\pi\bar{k}h^2. \tag{46}$$

This yields, for sufficiently large m, using (44), (45), (46) and $\eta_m + r_1(m, \eta_m) \to 0$ as $m \to \infty$,

$$-(\eta_m + r_1(m, \eta_m))\operatorname{Per}(\partial A) - 2\pi\bar{k}(\eta_m + r_1(m, \eta_m))^2 \leq \frac{3\sqrt{3}}{2} r_1(m, \eta_m)^2 m - \operatorname{Vol}(A) \leq 0$$

and then

$$\mathcal{R}(m, \eta_m) \leq r_1(m, \eta_m) - \left(\frac{2\operatorname{Vol}(A)}{3\sqrt{3}m}\right)^{1/2} \leq 0 \tag{47}$$

with

$$\mathcal{R}(m,\eta_m) := \frac{-2(\eta_m + r_1(m,\eta_m))\operatorname{Per}(\partial A) - 4\pi\bar{k}(\eta_m + r_1(m,\eta_m))^2}{3\sqrt{3}m\left(r_1(m,\eta_m) + \left(\frac{2\operatorname{Vol}(A)}{3\sqrt{3}m}\right)^{1/2}\right)}$$
$$= \frac{-2\operatorname{Per}(\partial A) - 4\pi\bar{k}(\eta_m + r_1(m,\eta_m))}{3\sqrt{3}}.$$

Using (47) we get

$$\mathcal{R}(m,\eta_m) \geq -\frac{2\operatorname{Per}(\partial A)}{3\sqrt{3}m} - \frac{8\pi\bar{k}\eta_m}{3\sqrt{3}m} = -\frac{2\operatorname{Per}(\partial A)}{3\sqrt{3}m} - \frac{8\pi\bar{k}(2\operatorname{Vol}(A))^{1/2}}{(3\sqrt{3}m)^{3/2}}. \tag{48}$$

This yields the result. $\square$

3.3 Asymptotic expansion of the optimal radius

In this section we show that the unique optimal covering of a honeycomb is obtained by covering each regular hexagon with a ball of radius equal to the maximal radius of the hexagon. For a set $C \subset \mathbb{R}^2$ and $\lambda > 0$, define $\lambda C := \{\lambda x \mid x \in C\}$ and the *translate* $y + C := \{y + x \mid x \in C\}$ of C. Let X be a discrete set of points in $\mathbb{R}^2$ and $\mathcal{K}$ a convex set, then $\mathcal{K} + X := \{x + y \mid x \in X, y \in \mathcal{K}\}$ is a *translative covering* of $\mathbb{R}^2$ if $\mathcal{K} + X = \mathbb{R}^2$. Let $S \subset \mathbb{R}^2$ be the unit square. When $\mathcal{K} + X$ is a covering of $\mathbb{R}^2$, we call

$$\Theta(\mathcal{K}, X) := \lim_{\lambda\to\infty} \frac{|\lambda S \cap X| \operatorname{Vol}(\mathcal{K})}{\operatorname{Vol}(\lambda S)}$$

the density of the covering, if the limit exists. Alternatively, in the definition of $\Theta(\mathcal{K}, X)$ one can replace the unit square S by any convex domain C, i.e.,

$$\Theta(\mathcal{K}, X) = \lim_{\lambda\to\infty} \frac{|\lambda C \cap X| \operatorname{Vol}(\mathcal{K})}{\operatorname{Vol}(\lambda C)}, \tag{49}$$

since any convex domain can be arbitrarily approximated by the union of a sequence of squares; see [40, Section 2].

Since the set to be covered in problem (1,2) is supposed to be open, we formulate the following result for the covering of the interior $\operatorname{int} H(L_r)$ of the honeycomb L_r, as $H(L_r)$ is defined as a closed set.

Theorem 4. *Let $L_r \subset \mathcal{L}_r$ be a sublattice satisfying $|L_r| = m$. Then the unique solution to the minimization problem*

$$\underset{(\boldsymbol{x},r)\in\mathbb{R}^{2m+1}}{\operatorname{Minimize}}\ r \quad \text{subject to} \quad \hat{G}(\boldsymbol{x}, r) = 0,$$

where $\hat{G}(\boldsymbol{x}, r) := \operatorname{Vol}(\operatorname{int} H(L_r)) - \operatorname{Vol}(\operatorname{int} H(L_r) \cap \Omega(\boldsymbol{x}, r))$, is given by $B(0, r) + L_r = \cup_{z\in L_r} B(z, r)$.

Proof. Clearly, the set $B(0, r) + L_r = \cup_{z\in L_r} B(z, r)$ is a covering of $\operatorname{int} H(L_r)$, so we just need to prove that this covering is optimal and unique. Suppose that there exists a discrete set Λ with $|\Lambda| = m$ such that $B(0, s) + \Lambda$, for some $s \leq r$, is a covering of $\operatorname{int} H(L_r)$. If $s < r$, then we must have $\Lambda \neq L_s$, since $B(0, s) + L_s$ can not be a covering of $\operatorname{int} H(L_r)$, and if $s = r$ we should also suppose $\Lambda \neq L_s$, thus we suppose that $\Lambda \neq L_s$ in any case. Since $s \leq r$, the set $B(0,r)+\Lambda$ is also a covering of $\operatorname{int} H(L_r)$.

For $p \in \mathbb{N}$ and $\mathbb{Z}_p^2 := \{(i,j) \in \mathbb{Z}^2 \mid |i| \leq p, |j| \leq p\}$, introduce the sublattice

$$\widehat{L}_p := \{kv_r + \ell w_r \mid (k,\ell) \in \mathbb{Z}_p^2\} \subset \mathcal{L}_r.$$

Clearly, there exists $p \in \mathbb{N}$ such that $L_r \subset \widehat{L}_p$. Further, there exists a tiling of $\mathcal{L}_r$ by a disjoint union of translates of $\widehat{L}_p$, indeed we have $\mathcal{L}_r = Y + \widehat{L}_p$ where $Y := \{y_{ij} \mid (i,j) \in \mathbb{Z}^2\}$, $y_{ij} := i(2p+1)v_r + j(2p+1)w_r$, and $\{y_{ij} + \widehat{L}_p\} \cap \{y_{k\ell} + \widehat{L}_p\} = \emptyset$ for all $(i,j) \neq (k,\ell)$.

Then $B(0,r) + \Lambda \cup (\widehat{L}_p \setminus L_r)$ is a covering of $\operatorname{int} H(\widehat{L}_p)$ since $B(0,r) + \widehat{L}_p \setminus L_r$ is a covering of $\operatorname{int} H(\widehat{L}_p \setminus L_r)$ and $B(0,r)+\Lambda$ is a covering of $\operatorname{int} H(L_r)$. Let us define

$$X := Y + \Lambda \cup (\widehat{L}_p \setminus L_r).$$

Then $B(0,r)+X$ is a covering of $\operatorname{int} H(Y+\widehat{L}_p) = \operatorname{int} H(\mathcal{L}_r) = \mathbb{R}^2$. Defining $Y_n := \{y_{ij} \mid (i,j) \in \mathbb{Z}_n^2\}$, the honeycomb $\operatorname{int} H(Y_n + \widehat{L}_p)$ can be approximated by the union of a sequence of squares, thus, in view of (49), the density of the covering $B(0,r)+X$ can be computed as

$$\begin{aligned}\Theta(B(0,r),X) &= \lim_{n\to\infty} \frac{|H(Y_n+\widehat{L}_p)\cap X| \operatorname{Vol}(B(0,r))}{\operatorname{Vol}(H(Y_n+\widehat{L}_p))}\\ &= \lim_{n\to\infty} \frac{(2n+1)^2 \pi r^2 |\Lambda \cup \widehat{L}_p \setminus L_r|}{(2n+1)^2(2p+1)^2 3\sqrt{3}r^2/2} \leq \frac{2\pi}{3\sqrt{3}},\end{aligned}$$

where we have used $|\Lambda \cup (\widehat{L}_p \setminus L_r)| \leq m + (2p+1)^2 - m = (2p+1)^2$, considering the fact that $\Lambda \cap (\widehat{L}_p \setminus L_r)$ may be nonempty. However, it is well-known that

$$\Theta(B(0,r)) = \inf_{\mathcal{X}} \Theta(B(0,r),\mathcal{X}) = \frac{2\pi}{3\sqrt{3}}$$

and that this bound is attained only when the centers of the discs are arranged in a regular hexagonal lattice, see [15, Chapter 2, p. 32]. The set X is not a regular hexagonal lattice since $\Lambda \neq L_r$. Thus we have obtained a contradiction, which means that Λ does not exist. Thus the covering $B(0,r)+L_r$ is indeed optimal and unique. $\square$

3.4 Proof of Theorem 1

We have shown in Theorem 2 that $A \subset H(L_0(m,\mu_m))$ for $m \geq m_0$ with $m_0 \geq \frac{16\pi\bar{k}}{3\sqrt{3}}$, which implies $A \subset \operatorname{int} H(L_0(m,\mu_m))$ since A is open. Thus any covering of $\operatorname{int} H(L_0(m,\mu_m))$ also covers A. According to Theorem 4, the optimal covering of $\operatorname{int} H(L_0(m,\mu_m))$ is given by $B(z, r_0(m,\mu_m)) + L_0(m,\mu_m)$, this shows that $r^*(m) \leq r_0(m,\mu_m)$.

We have also shown in Theorem 3 that $H(L_1(m,\eta_m)) \subset \overline{A}$ for $m \geq m_1$ with $m_1 \geq \frac{4\pi\bar{k}}{3\sqrt{3}}$. Since $A \subset \Omega(\boldsymbol{x}^*(m), r^*(m))$, where $(\boldsymbol{x}^*(m), r^*(m))$ is a solution of (1,2), we also have $\overline{A} \subset \overline{\Omega(\boldsymbol{x}^*(m), r^*(m))}$, hence $H(L_1(m,\eta_m)) \subset \overline{\Omega(\boldsymbol{x}^*(m), r^*(m))}$ and

$$\operatorname{int} H(L_1(m,\eta_m)) \subset \operatorname{int} \overline{\Omega(\boldsymbol{x}^*(m), r^*(m))}.$$

This yields, in view of the definition of $\hat{G}(\boldsymbol{x}, r)$ in Theorem 4,

$$\begin{aligned}\hat{G}(\boldsymbol{x}^*(m), r^*(m)) &= \mathrm{Vol}(\mathrm{int}\, H(L_1(m,\eta_m))) - \mathrm{Vol}(\mathrm{int}\, H(L_1(m,\eta_m)) \cap \Omega(\boldsymbol{x}^*(m), r^*(m))) \\ &= \mathrm{Vol}(\mathrm{int}\, H(L_1(m,\eta_m))) - \mathrm{Vol}(\mathrm{int}\, H(L_1(m,\eta_m)) \cap \mathrm{int}\, \overline{\Omega(\boldsymbol{x}^*(m), r^*(m))}) \\ &= 0.\end{aligned}$$

Then, according to Theorem 4, the covering of $\mathrm{int}\, H(L_1(m,\eta_m))$ given by $B(0, r_1(m,\eta_m)) + L_1(m,\eta_m)$ is optimal, this shows that $r_1(m,\eta_m) \le r^*(m)$.

Thus we have shown

$$\left[\frac{2\,\mathrm{Vol}(A)}{3\sqrt{3}m}\right]^{1/2} + R_1(m) = r_1(m,\eta_m) \le r^*(m) \le r_0(m,\mu_m) = \left[\frac{2\,\mathrm{Vol}(A)}{3\sqrt{3}m}\right]^{1/2} + R_0(m).$$

Using Theorems 2 and 3 we obtain (19). Finally, choosing $\overline{m} := \max\{m_0, m_1\}$, where m_0, m_1 are given in Theorems 2 and 3, we obtain (20).

4 Heuristic generation of lattice-based initial guesses

The covering problem was formulated in (1,2) as a nonlinear programming problem that has a very large number of stationary points, most of which do not represent solutions to the covering problem. In [9, 10], a local minimization method was combined with a multi-start technique to increase the chance of finding a global solution to the problem. The way of generating starting points was simple and did not make use of problem-specific and observable features in the solutions found. As a consequence, a large number of local minimizations were needed to find good quality solutions.

In this section, two characteristics of the solutions are explored in order to develop a method to generate better quality random starting points. On the one hand, when the number of balls is large, in a solution, the balls in the interior of the region A to be covered tend to be organized in the form of an hexagonal lattice, as demonstrated in Section 3. On the other hand, when a ball does not intersect the region A, the partial derivatives relative to its center are null. Thus, if a ball does not intersect A in the initial solution, unless throughout the optimization process the radius increases and causes the ball to intersect A, the ball will remain where it is, not contributing to the final covering. With fewer balls contributing, the solution found tends to be sub-optimal.

We describe below a way to generate lattice-like initial solutions. The general idea is to cover the region A with m balls whose arrangement resembles that of a hexagonal lattice. The conditions are that: (a) there are exactly m balls, (b) there is no ball having empty intersection with A, and (c) the balls cover A in a "minimally reasonable way".

Given $m \ge 1$ and $\kappa \in (0,1]$, we say that $r > 0$ makes the lattice $\mathcal{L}_r$ to be (m,κ)-admissible (as a lattice able to produce a useful initial guess for the optimization process) if there exists a displacement $d \in \mathbb{R}^2$ and a rotation angle θ such that

$$|C(\mathcal{L}_r, d, \theta)| \ge m, \tag{50}$$

where

$$C(\mathcal{L}_r, d, \theta) := \left\{ x \in \mathbb{R}^2 \;\middle|\; x = d + R_\theta\, c,\ c \in \mathcal{L}_r,\ \text{and}\ \frac{\mathrm{Vol}(B(x,r) \cap A)}{\mathrm{Vol}(B(x,r))} \ge \kappa \right\}$$

and

$$R_\theta := \begin{pmatrix} \cos\theta & -\sin\theta \\ \sin\theta & \cos\theta \end{pmatrix}.$$

In other words, given a displacement d and a rotation angle θ, a point $d + R_\theta c$ with $c \in \mathcal{L}_r$ is part of $C(\mathcal{L}_r, d, \theta)$ if at least $100\% \times \kappa$ of the ball of radius r centered at $d + R_\theta c$ covers A. Accordingly, roughly speaking, being (m, κ)-admissible means that the lattice $\mathcal{L}_r$ can be associated with at least m balls that are "useful" to cover A. Regardless of d and θ, if r is sufficiently large, we have $|C(\mathcal{L}_r, d, \theta)| \approx 1$ and $\mathcal{L}_r$ probably inadmissible; while if r is sufficiently small we have $|C(\mathcal{L}_r, d, \theta)|$ large and $\mathcal{L}_r$ certainly admissible. Given m and κ, the interesting r is the largest r that makes $\mathcal{L}_r$ to be (m, κ)-admissible.

Let $v_{\rm bl}(A)$ be the "bottom-left corner" of $\overline{A}$ defined as the point in $\overline{A}$ with the lowest ordinate and, in case of a tie, that with the lowest abscissa. To determine empirically whether r makes $\mathcal{L}_r$ to be (m, κ)-admissible, we draw $d \in B(v_{\rm bl}(A), r)$ and $\theta \in [0, \pi)$ up to 100 times and, by constructing $C(\mathcal{L}_r, d, \theta)$, check whether (50) holds. If we find d and θ such that (50) holds, we say that the answer is "yes". Otherwise we say that the answer is "no". Figure 2 illustrates the output of this process.

Empirically, we define an interval $[r_{\rm left}, r_{\rm right}]$ and we obtain by bisection in that interval, the largest r for which we can show that it makes $\mathcal{L}_r$ to be (m, κ)-admissible. We stop the bisection process when $(r_{\rm right} - r_{\rm left})/r_{\rm left} \le r_\epsilon := 10^{-2}$. We denote by $\bar{r}$ the r found and denote by $\bar{d}$ and $\bar{\theta}$ the displacement and angle that show that $\mathcal{L}_{\bar{r}}$ is (m, κ)-admissible. Up to this point, we constructed, as a rotation and translation of a subset of points of the lattice $\mathcal{L}_{\bar{r}}$, the set $C(\mathcal{L}_{\bar{r}}, \bar{d}, \bar{\theta})$ with at least m points such that, for all $x \in C(\mathcal{L}_{\bar{r}}, \bar{d}, \bar{\theta})$, the ball of center x and radius $\bar{r}$ uses at least $100 \times \kappa$ percent of its area to cover A. To complete the construction of an initial guess for the optimization process, it remains to perturb the points in $C(\mathcal{L}_{\bar{r}}, \bar{d}, \bar{\theta})$ and eliminate some points if we have more than m.

For each $x \in C(\mathcal{L}_{\bar{r}}, \bar{d}, \bar{\theta})$, we compute $d(x, \partial A)$, i.e. its distance to the boundary of A. Let $d_{\max} := \max_{x \in C(\mathcal{L}_{\bar{r}}, \bar{d}, \bar{\theta})} \{d(x, \partial A)\}$. For each x, we consider a perturbation that is inversely proportional to $d(x, \partial A)/d_{\max}$, i.e. we perturb more the centers near the edges of A and less the x in the interior of A. Precisely, given $0 \le \sigma_1 \le \sigma_2 \le 1$, we define $\gamma(x) := \sigma_1 + (\sigma_2 - \sigma_1)(1 - d(x, \partial A)/d_{\max})$ and replace x by a random point in the box centered at x with half-side $\gamma(x)\bar{r}$. (In the numerical experiments we arbitrarily considered $\sigma_1 = 0.03$ and $\sigma_2 = 0.15$.) With abuse of notation, we continue to call $C(\mathcal{L}_{\bar{r}}, \bar{d}, \bar{\theta})$ the set of perturbed points. Finally, if we have in $C(\mathcal{L}_{\bar{r}}, \bar{d}, \bar{\theta})$ more than m elements, we calculate $\mathrm{Vol}(B(x, \bar{r}) \cap A)$ and eliminate the points $x \in C(\mathcal{L}_{\bar{r}}, \bar{d}, \bar{\theta})$ with smaller useful area.

If we wish to generate $n_{\rm trial}$ different initial guesses for the problem of covering a region A with m balls, then we perform the whole procedure described above $n_{\rm trial}$ times for random values of κ. In the experiments, we arbitrarily considered values of κ in $[0.1, 0.9]$.

5 Numerical experiments

In this section, we wish to illustrate with numerical experiments (i) the theoretical properties of optimal solutions introduced in Section 3 and (ii) the heuristic for the generation of initial solutions introduced in Section 4. Moreover, extensive numerical experiments of covering regular polygons are presented.

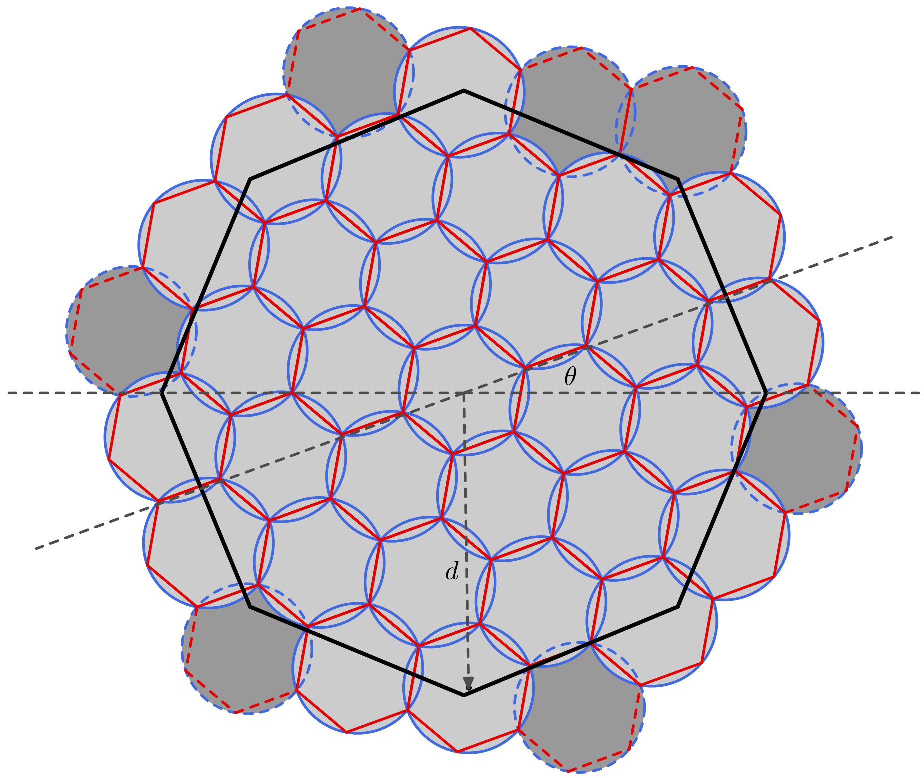

Figure 2: Region A is given by an octagon with its vertices in a unitary-radius ball. In this example, we consider $m = 30$, $\kappa = 0.3$, and $r \approx 0.215$. The figure shows a displacement $d \approx (0.0156, -0.97542)^T$ and an angle $\theta \approx 0.35$ such that $|C(\mathcal{L}_r, d, \theta)| = m$, i.e. d and θ which show that $\mathcal{L}_r$ is (m, κ)-admissible. Balls in the figure are all the balls that intersect A and such that their centers are rotated and translated elements of $\mathcal{L}_r$. The figure shows in light gray the balls whose centers belong to $C(\mathcal{L}_r, d, \theta)$ and with dark gray balls whose centers do not belong $C(\mathcal{L}_r, d, \theta)$. Recall that, by definition, to belong to $C(\mathcal{L}_r, d, \theta)$ a ball must use at least $100 \times \kappa$ percent of its area to cover A.

Following [10], the nonlinear programming problem (1,2) is tackled with the Augmented Lagrangian optimization method Algencan [1, 11, 12]. As usual, to find good quality solutions, we use a multi-start strategy. The procedure as a whole consists of (a) generating random initial points, (b) using the initial points to solve the problem with Algencan, and (c) reporting the best local solution obtained as the final solution. Algencan was used with all its default parameters. This means, in particular, that for all reported solutions $(\boldsymbol{x}^*, r^*)$ it is valid that $G(\boldsymbol{x}^*, r^*) \leq 10^{-8}$.

Algencan 4.0, implemented in Fortran 90, is freely available at `http://www.ime.usp.br/~egbirgin/`. The constraint $G(\boldsymbol{x}, r)$ defined in (2), as well as its first- and second-order derivatives, were also implemented in Fortran 90; see Algorithms 1, 2, and 3 in [10]. The implementation considers that the region A to be covered is given by the union of non-overlapping convex polygons $A_1, \dots, A_p$. Implementing the algorithms that computes G and its derivatives requires the calculation of the Voronoi diagram associated with the balls centers $\{x_i\}_{i=1}^m$, that is calculated with subroutine `dtris2` from Geompack. (In fact, `dtris2` provides a Delaunay triangulation from which the Voronoi diagram is extracted.) The intersection W_{ij} of each Voronoi cell V_i (that is a bounded or unbounded polyhedron) and each convex polygon A_j is computed with the Sutherland-Hodgman algorithm [35]. Finally, the intersection S_{ij} of W_{ij} with the ball $B(x_i, r)$ is computed with an adaptation of a single iteration of the Sutherland-Hodgman algorithm; see [10]. From these structures, the values of G and its first- and second-order derivatives at a given point $(\boldsymbol{x}, r)$ are obtained.

Source code necessary to reproduce all numerical experiments presented in this section is available at `https://github.com/johngardenghi/bglcovering`. All tests were conducted on a computer with an Intel Core i7-8700 processor and 16GB of RAM memory, running Ubuntu GNU/Linux (version 20.04.3 LTS). Code was compiled by the GFortran compiler of GCC (version 9.3.0) with the -O3 optimization directive enabled.

5.1 Verifying theoretical properties

In this section, we first consider the problem of covering an equilateral triangle with its vertices in a unitary-radius ball considering increasing values of m. For each value of m, a budget of $n_{\text{trials}} = 1000$ starting points was considered. If we call $r_i^*(m)$ the radius found starting from the ith starting point, hereafter we use $r^*(m)$ to refer to $r^*(m) := \min_{\{i=1,\dots,n_{\text{trials}}\}}\{r_i^*(m)\}$. Figure 3 displays $r^*(m)$ along with its lower and upper bounds and its asymptotic upper bound. The figure shows that numerically computed radii are within their bounds. The relative distance from $r^*(m)$ to the lower bound gives us a guarantee of the distance to the optimal value. For example, for $m = 200$, $(r^*(m) - \text{LB}(m))/\text{LB}(m) \approx 0.41$, where $\text{LB}(m) = (2\,\text{Vol}(A)/(3\sqrt{3}m))^{1/2} + \underline{R}(m)$; see Theorem 1. This means that the calculated radius is, in the worst case, 41% larger than the optimal radius. In the case $m = 1000$, the distance to the optimum radius is, in the worst case, 13%. For values of m not greater than 90, these percentages are greater than 100%.

In Figure 4 we compare the theoretical convergence rate $2\,\text{Per}(\partial A)/(3\sqrt{3}m)$ of the upper bound of $|R(m)|$, as given in Theorem 1, with the numerical convergence rate of $|R(m)|$. We observe that the theoretical and numerical rates are similar. Note that in this particular case, the absolute value of the remainder $|R(m)|$ is dominated by the positive part of $R(m)$, as the numerical results yield $\min\{R(m), 0\} = 0$. This indicates that in the case of the equilateral triangle, the main asymptotic term in the expansion of $\overline{R}(m)$ in Theorem 1 could possibly be improved by a multiplicative constant, while a sharp lower bound could have a higher order than the order m^{-1} given by Theorem 1. Nevertheless, since the results of Theorem 1 are valid for a large class of sets A, the bounds represent a worst-case scenario, hence it is not clear if these bounds can be improved for this class of sets A.

We further investigate this question by plotting the ratio $|R(m)|/(2\,\text{Per}(\partial A)/(3\sqrt{3}m))$ for four different sets A in Figure 5. In all four cases, this ratio seems to numerically converge towards a constant C_0 with the approximate values $C_0 \approx 0.22$ for the pentagon, $C_0 \approx 0.21$ for the octagon, and $C_0 \approx 0.20$ for the sets "Cèsaro Fractal" and "Non-convex with holes". This indicates that the main asymptotic term in the expansion of $\overline{R}(m)$ in Theorem 1 could possibly be improved by a multiplicative constant $1 > C_0 > 0.22$. Additional numerical experiments for other shapes A would allow to determine a more precise target values for C_0, either for a general class of sets A or for specific shapes, and will be the topic of future investigations.

5.2 Comparison with random initial guesses

In this section, we present experiments to show that lattice-based starting points are more effective and efficient, to produce good quality solutions, than the random starting points considered in [10].

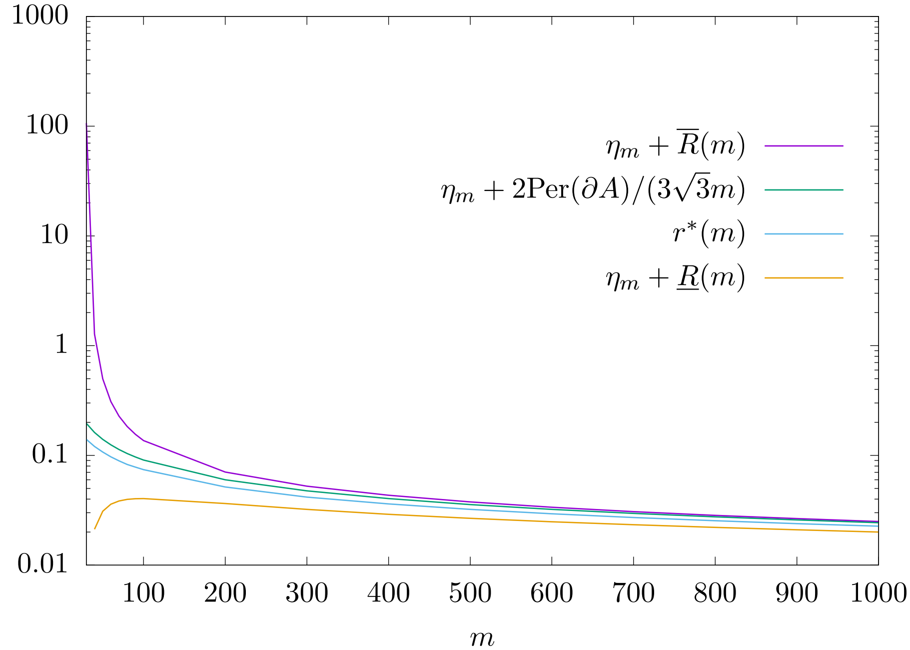

Figure 3: Illustration of $r^*(m)$ (presumably close to optimal) best radii computed for an equilateral triangle and $m \in \{30, 40, \dots, 100, 200, \dots, 1000\}$, together with its bounds $\eta_m + \underline{R}(m)$, $\eta_m + \overline{R}(m)$, and $\eta_m + 2\,\mathrm{Per}(\partial A)/(3\sqrt{3}m)$, with $\eta_m = (2\,\mathrm{Vol}(A)/3\sqrt{3}m)^{1/2}$ (see Theorem 3). The picture starts at $m = 30$ considering that Theorem 1 requires $m > \overline{m} \geq 16\pi\bar{k}/(3\sqrt{3})$ and $16\pi\bar{k}/(3\sqrt{3}) = 16\pi/\sqrt{3} \approx 29.02$ in the case of a triangle (i.e., $\bar{k} = 3$). The curve of the lower bound $\eta_m + \underline{R}(m)$ starts at $m = 40$ because it assumes negative value when $m = 30$.

For this purpose, we consider the three regions A and the number of balls $m \in \{10, 20, \dots, 100\}$ considered in [10, Table 1], totaling 30 different experiments. The two ways of generating initial points were compared for increasing values of budgets, where by "budget" we mean the number n_{trials} of different initial points considered in the multi-start procedure. Tables 1, 2, and 3 show the results for problems "Non-convex with holes", "Cesàro fractal", and "Sketch of America", respectively. In the tables, results with budget $n_{\text{trials}} \in \{200, 500, 1000, 2000, 5000, 10\,000\}$ are shown. For each value of n_{trials} and each number of balls m, the tables show the best radius r^* found when the lattice-based initial guesses are used. Tables also show the relative gap $e(r^*) := (\bar{r} - r^*)/\bar{r}$, where $\bar{r}$ is the best radius found in [10], in which random initial guesses were considered. A positive value of $e(r^*)$ indicates the radius found in the present work was better (i.e., smaller) than the one found in [10]. For each r^*, the tables also show which initial guess (between 1 and n_{trials}) was the one that made the optimization method to reach r^*. Finally, let $n_{\text{trials}}^{\text{prev}}$ and n_{trials} satisfying $n_{\text{trials}}^{\text{prev}} < n_{\text{trials}}$ be two consecutive budgets in $\{200, 500, 1000, 2000, 5000, 10\,000\}$; and let r^*_{prev} and r^* be the associated best radii found. The tables show the relative improvement $i(r^*) = (r^* - r^*_{\text{prev}})/r^*_{\text{prev}}$, non-negative by definition. This improvement reflects how much profitable it was to increase the budget.

Let us concentrate on the results of Table 1 (Tables 2 and 3 show similar results). In 19 out of the 60 combinations of n_{trials} and m, $e(r^*)$ is negative, meaning that the solution found in the present

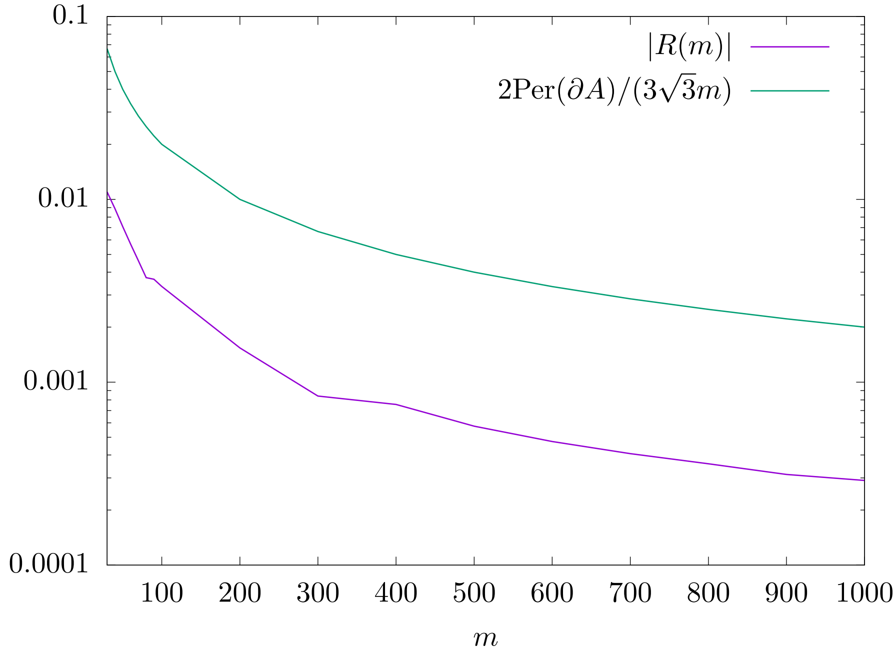

Figure 4: Comparison of theoretical convergence rate $2\,\mathrm{Per}(\partial A)/(3\sqrt{3}m)$ of the upper bound of $|R(m)|$ (see Theorem 1), and the numerical convergence rate of $|R(m)|$, for the covering of an equilateral triangle. We observe that the theoretical and numerical rates are similar.

work was worse than the solution found in [10]. However, 18 out these 19 combinations correspond to $m = 10, 20, 30$ and only one corresponds to $m = 40$. This means that, as expected, in the smaller problems, in which solutions do not exhibit a lattice-like arrangement, using random initial guesses is better. On the other hand, in the other 41 combinations (out of 60), all corresponding to the larger instances, the lattice-like initial guesses yield better solutions. In average, solutions were better for all considered budgets. For the largest considered budget ($n_{\text{trials}} = 10\,000$), improvements $i(r^*)$ are null for all m. This means that increasing the budget from 5000 to 10 000 did not improve any result. Therefore, the new approach is able to improve the quality of the solutions found with random initial guesses for values of m between 50 and 100 using at least half of the effort. For smaller problems, it seems that random initial guesses are still preferable.

5.3 Covering regular polygons

In this section, we apply the techniques introduced in this paper and in [9, 10] to produce regular polygon coverings. Coverings of equilateral triangles and squares were already considered in [14, 16, 27, 31] and [16, 28, 32, 34], respectively. Results with $m \leq 9$ for the case of equilateral triangles and $m \leq 12$ for the case of squares can be found at `https://erich-friedman.github.io/packing/index.html` (accessed on February 9th, 2022). All results with m up to 36 for triangles and m up to 30 for squares were gathered in [31, 32]. Comparing with them, we assert the quality of the solutions found by the proposed method. Table 4 shows the results. In the table, r^* corresponds to the radii found in the present work, while $e_{\text{abs}}(r^*) = (\bar{r} - r^*)$ and $e_{\text{rel}} = e_{\text{abs}}(r^*)/\bar{r}$ correspond to the absolute and relative difference to the best radius $\bar{r}$ obtained using the algorithm in [31, 32],

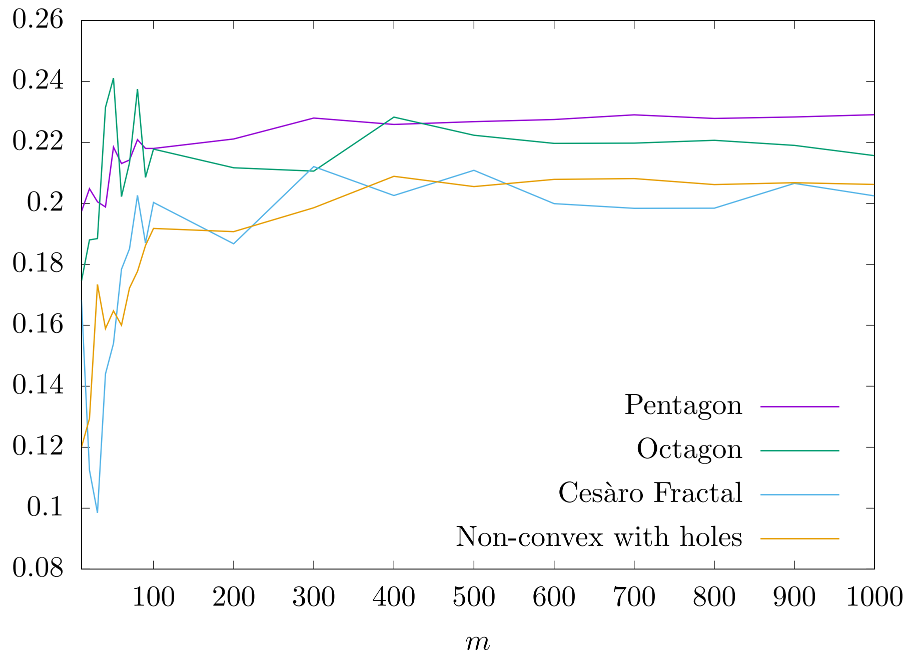

Figure 5: Values of the ratio $|R(m)|/(2\,\mathrm{Per}(\partial A)/(3\sqrt{3}m))$ as m grows for four arbitrary problems considered in this work. In this picture, we can notice that the ratio converges to a constant C_0 that approximately holds 0.22 (Pentagon), 0.21 (Octagon), and 0.20 (both Cesàro Fractal and Non-convex with holes), which may indicate that we can improve the upper bound $\overline{R}(m)$ (see Theorem 1) in a factor of C_0 for these particular sets.

respectively (i.e. the values shown in [31, 32, Table 1]). Positive values of $e_{\{\text{abs,rel}\}}(r^*)$ correspond to better solutions found with the lattice-based initial guesses. The left side of the table shows that all 36 differences are positive in the case of triangles, while the right side of the table shows that differences are positive in 27 out the 30 instances with squares. All positive absolute differences are of the order of 10^{-5} or 10^{-6}.

At this point, a clarification regarding the accuracy of the solutions obtained would be appropriate. In Nurmela's work [31, 32] as well as in the other papers to which it refers, iterative optimization methods such as the one being used in this paper are used. All these methods generate a sequence of approximations to a solution and are stopped when some stopping criterion is satisfied, assuming that they have arrived sufficiently close to the desired solution. The reasonableness of the used stopping tolerance depends on the problem, i.e., on the way the feasibility is measured, the size of the region to be covered and the units of measurement considered. By that, we mean that getting a positive (or negative) difference of 10^{-5} does not necessarily mean that we found a better (or worse) solution. It probably means that the methods were stopped with slightly different tolerances. The important thing is that, as in previous work, these solutions can be used to detect the structure of the solution and, with some other method with a higher convergence rate, if desired, improve its accuracy; see [7, 36]. The idea consists of assembling a system of nonlinear equations which is then solved with some method for nonlinear systems. The nonlinear system described in [32] includes constraints stating that the distance from the center of

m	Up to 200 trials				Up to 500 trials				Up to 1000 trials			
	r^*	$e(r^*)$	trial	$i(r^*)$	r^*	$e(r^*)$	trial	$i(r^*)$	r^*	$e(r^*)$	trial	$i(r^*)$
10	1.95466310e−01	−3.890e−12	8	–	1.95466310e−01	−3.890e−12	8	0.000e+00	1.95466310e−01	−3.890e−12	8	0.000e+00
20	1.33726730e−01	−7.151e−03	3	–	1.32777211e−01	−1.999e−12	347	7.100e−03	1.32777211e−01	−1.999e−12	347	0.000e+00
30	1.09757874e−01	−1.461e−03	53	–	1.09757874e−01	−1.461e−03	53	0.000e+00	1.09757874e−01	−1.461e−03	53	0.000e+00
40	9.22659297e−02	6.537e−03	9	–	9.22659297e−02	3.267e−03	9	0.000e+00	9.22659297e−02	1.796e−03	9	0.000e+00
50	8.21716544e−02	4.739e−03	76	–	8.21716544e−02	3.303e−03	76	0.000e+00	8.18281777e−02	7.469e−03	606	4.180e−03
60	7.40371358e−02	9.959e−03	159	–	7.40042018e−02	4.927e−03	426	4.448e−04	7.37792389e−02	7.952e−03	542	3.040e−03
70	6.82811133e−02	1.712e−02	131	–	6.82811133e−02	1.635e−02	131	0.000e+00	6.82811133e−02	1.503e−02	131	0.000e+00
80	6.41308713e−02	1.426e−02	180	–	6.37828293e−02	1.961e−02	334	5.427e−03	6.36555134e−02	7.878e−03	723	1.996e−03
90	5.99463942e−02	2.157e−02	154	–	5.99463942e−02	1.470e−02	154	0.000e+00	5.99463942e−02	1.470e−02	154	0.000e+00
100	5.68950205e−02	1.207e−02	106	–	5.67505517e−02	1.081e−02	251	2.539e−03	5.67493227e−02	1.083e−02	875	2.166e−05
Average		7.765e−03		–		7.150e−03		1.551e−03		6.419e−03		9.238e−04

m	Up to 2000 trials				Up to 5000 trials				Up to 10 000 trials			
	r^*	$e(r^*)$	trial	$i(r^*)$	r^*	$e(r^*)$	trial	$i(r^*)$	r^*	$e(r^*)$	trial	$i(r^*)$
10	1.95466310e−01	−4.034e−12	8	0.000e+00	1.95466310e−01	−4.246e−12	8	0.000e+00	1.95466310e−01	−1.331e−11	8	0.000e+00
20	1.32777211e−01	−1.999e−12	347	0.000e+00	1.32777211e−01	−2.261e−12	347	0.000e+00	1.32777211e−01	−2.261e−12	347	0.000e+00
30	1.09757874e−01	−1.461e−03	53	0.000e+00	1.09757874e−01	−1.461e−03	53	0.000e+00	1.09757874e−01	−2.816e−03	53	0.000e+00
40	9.22659297e−02	1.109e−03	9	0.000e+00	9.21104165e−02	1.685e−03	3384	1.685e−03	9.21104165e−02	−1.245e−11	3384	0.000e+00
50	8.16364785e−02	7.820e−03	1155	2.343e−03	8.15511636e−02	6.197e−03	4147	1.045e−03	8.15511636e−02	6.197e−03	4147	0.000e+00
60	7.37792389e−02	7.952e−03	542	0.000e+00	7.37792389e−02	6.521e−03	542	0.000e+00	7.37792389e−02	2.613e−03	542	0.000e+00
70	6.82811133e−02	1.420e−02	131	0.000e+00	6.82336187e−02	1.046e−02	3715	6.956e−04	6.82336187e−02	1.046e−02	3715	0.000e+00
80	6.36555134e−02	7.878e−03	723	0.000e+00	6.36555134e−02	7.878e−03	723	0.000e+00	6.36555134e−02	6.397e−03	723	0.000e+00
90	5.99463942e−02	1.470e−02	154	0.000e+00	5.99463942e−02	6.619e−03	154	0.000e+00	5.99463942e−02	6.619e−03	154	0.000e+00
100	5.67493227e−02	1.083e−02	875	0.000e+00	5.66690709e−02	9.741e−03	3539	1.414e−03	5.66690709e−02	9.741e−03	3539	0.000e+00
Average		6.302e−03		2.343e−04		4.764e−03		4.840e−04		3.921e−03		0.000e+00

Table 1: Comparison of the best radii found for the problem "Non-convex with holes" when the initial guesses are random, like in [10], and when the proposed lattice-like initial guesses are considered.

m	Up to 200 trials				Up to 500 trials				Up to 1000 trials			
	r^*	$e(r^*)$	trial	$i(r^*)$	r^*	$e(r^*)$	trial	$i(r^*)$	r^*	$e(r^*)$	trial	$i(r^*)$
10	2.12768646e−01	4.190e−06	66	–	2.12768646e−01	−1.096e−12	66	0.000e+00	2.12768646e−01	−1.096e−12	66	0.000e+00
20	1.33268785e−01	−3.580e−10	1	–	1.33268785e−01	−1.502e−09	1	0.000e+00	1.33268785e−01	−1.502e−09	1	0.000e+00
30	1.05235228e−01	4.383e−09	70	–	1.05235228e−01	4.383e−09	70	0.000e+00	1.05235220e−01	8.236e−08	896	7.798e−08
40	9.32071842e−02	9.521e−03	75	–	9.32071842e−02	6.697e−03	75	0.000e+00	9.32071842e−02	6.266e−03	75	0.000e+00
50	8.30039792e−02	1.375e−02	167	–	8.29835509e−02	1.399e−02	257	2.461e−04	8.29835509e−02	9.313e−03	257	0.000e+00
60	7.64998086e−02	2.576e−02	52	–	7.61937155e−02	2.965e−02	291	4.001e−03	7.61937155e−02	2.965e−02	291	0.000e+00
70	7.02452018e−02	1.360e−02	130	–	7.02452018e−02	7.041e−03	130	0.000e+00	7.02452018e−02	7.041e−03	130	0.000e+00
80	6.59479847e−02	1.575e−02	10	–	6.58705734e−02	1.636e−02	276	1.174e−03	6.58705734e−02	1.131e−02	276	0.000e+00
90	6.14009288e−02	2.361e−02	145	–	6.12535832e−02	2.595e−02	204	2.400e−03	6.12535832e−02	2.428e−02	204	0.000e+00
100	5.82836412e−02	1.607e−02	198	–	5.82836412e−02	1.506e−02	198	0.000e+00	5.81992746e−02	1.409e−02	702	1.448e−03
Average		1.686e−03		–		1.639e−03		1.117e−04		1.457e−03		2.068e−05

m	Up to 2000 trials				Up to 5000 trials				Up to 10 000 trials			
	r^*	$e(r^*)$	trial	$i(r^*)$	r^*	$e(r^*)$	trial	$i(r^*)$	r^*	$e(r^*)$	trial	$i(r^*)$
10	2.12768646e−01	−4.895e−12	66	0.000e+00	2.12768646e−01	−1.089e−11	66	0.000e+00	2.12768646e−01	−5.623e−11	66	0.000e+00
20	1.33268785e−01	−1.502e−09	1	0.000e+00	1.33268785e−01	−9.714e−09	1	0.000e+00	1.33268780e−01	2.177e−08	5210	3.464e−08
30	1.05235220e−01	7.781e−08	896	0.000e+00	1.05231934e−01	3.130e−05	2260	3.122e−05	1.05231921e−01	−9.774e−05	6514	1.280e−07
40	9.32071842e−02	6.266e−03	75	0.000e+00	9.32071842e−02	2.364e−03	75	0.000e+00	9.32071842e−02	2.364e−03	75	0.000e+00
50	8.29832289e−02	3.972e−03	1587	3.880e−06	8.29721218e−02	4.106e−03	2386	1.338e−04	8.29721218e−02	4.106e−03	2386	0.000e+00
60	7.61937155e−02	2.965e−02	291	0.000e+00	7.61417405e−02	2.986e−02	2840	6.821e−04	7.59122527e−02	3.019e−02	6602	3.014e−03
70	7.02368469e−02	7.159e−03	1615	1.189e−04	7.01584274e−02	4.634e−03	3830	1.117e−03	7.01584274e−02	4.287e−03	3830	0.000e+00
80	6.58705734e−02	5.568e−03	276	0.000e+00	6.58308578e−02	6.168e−03	3795	6.029e−04	6.58308578e−02	4.234e−03	3795	0.000e+00
90	6.12378326e−02	1.950e−02	1270	2.571e−04	6.12378326e−02	1.950e−02	1270	0.000e+00	6.12377271e−02	1.160e−02	7366	1.722e−06
100	5.81343527e−02	6.616e−03	1309	1.116e−03	5.80625691e−02	6.900e−03	2795	1.235e−03	5.80625691e−02	6.900e−03	2795	0.000e+00
Average		1.125e−03		2.136e−05		1.051e−03		5.431e−05		9.083e−04		4.308e−05

Table 2: Comparison of the best radii found for the problem "Cesàro fractal" when the initial guesses are random, like in [10], and when the proposed lattice-like initial guesses are considered.

a ball to certain other points must be equal to r, with r variable but equal for all distances. Those other points are the points where the ball intersects with two other balls simultaneously, or with

m	Up to 200 trials				Up to 500 trials				Up to 1000 trials			
	r^*	$e(r^*)$	trial	$i(r^*)$	r^*	$e(r^*)$	trial	$i(r^*)$	r^*	$e(r^*)$	trial	$i(r^*)$
10	1.11645171e−01	−8.042e−10	15	–	1.11645171e−01	−8.042e−10	15	0.000e+00	1.11645171e−01	−8.244e−03	15	0.000e+00
20	7.08273711e−02	8.325e−03	8	–	7.05661937e−02	3.688e−03	331	3.688e−03	7.05661937e−02	4.287e−11	331	0.000e+00
30	5.72425828e−02	−1.314e−03	96	–	5.69149299e−02	5.903e−04	425	5.724e−03	5.69149299e−02	5.903e−04	425	0.000e+00
40	4.90956074e−02	1.303e−02	130	–	4.90956074e−02	1.303e−02	130	0.000e+00	4.90956074e−02	−9.639e−03	130	0.000e+00
50	4.34368652e−02	1.247e−02	19	–	4.34368652e−02	3.575e−03	19	0.000e+00	4.33225166e−02	6.198e−03	603	2.633e−03
60	3.94093506e−02	1.750e−02	118	–	3.88806601e−02	1.240e−02	207	1.342e−02	3.86923093e−02	1.467e−02	947	4.844e−03
70	3.53960463e−02	2.009e−02	175	–	3.53960463e−02	1.061e−02	175	0.000e+00	3.53960463e−02	5.711e−03	175	0.000e+00
80	3.36138570e−02	1.898e−02	175	–	3.28948275e−02	3.557e−02	325	2.139e−02	3.28948275e−02	2.509e−02	325	0.000e+00
90	3.13138458e−02	3.090e−03	163	–	3.12276358e−02	5.834e−03	206	2.753e−03	3.12276358e−02	2.541e−03	206	0.000e+00
100	2.96369517e−02	6.813e−03	58	–	2.96369517e−02	6.813e−03	58	0.000e+00	2.91721038e−02	1.422e−02	858	1.568e−02
Average		1.414e−03		–		1.316e−03		6.710e−04		7.305e−04		3.309e−04

m	Up to 2000 trials				Up to 5000 trials				Up to 10 000 trials			
	r^*	$e(r^*)$	trial	$i(r^*)$	r^*	$e(r^*)$	trial	$i(r^*)$	r^*	$e(r^*)$	trial	$i(r^*)$
10	1.11645171e−01	−8.244e−03	15	0.000e+00	1.11645171e−01	−1.287e−02	15	0.000e+00	1.10732305e−01	−4.586e−03	9431	8.176e−03
20	7.05661937e−02	4.287e−11	331	0.000e+00	7.05661937e−02	6.872e−12	331	0.000e+00	7.05661937e−02	6.872e−12	331	0.000e+00
30	5.66536407e−02	5.178e−03	1286	4.591e−03	5.66536407e−02	5.178e−03	1286	0.000e+00	5.66320690e−02	−4.976e−03	6464	3.808e−04
40	4.89710085e−02	−7.077e−03	1153	2.538e−03	4.87387053e−02	−2.299e−03	4764	4.744e−03	4.84156015e−02	1.415e−03	9411	6.629e−03
50	4.29520825e−02	1.470e−02	1361	8.551e−03	4.29520825e−02	3.146e−03	1361	0.000e+00	4.29520825e−02	2.961e−03	1361	0.000e+00
60	3.86923093e−02	3.198e−03	947	0.000e+00	3.86758794e−02	8.700e−04	4113	4.246e−04	3.83522944e−02	8.196e−03	5918	8.367e−03
70	3.51217916e−02	1.112e−02	1713	7.748e−03	3.50628371e−02	1.174e−02	3847	1.679e−03	3.50628371e−02	1.174e−02	3847	0.000e+00
80	3.28948275e−02	1.397e−02	325	0.000e+00	3.28460358e−02	7.986e−03	2604	1.483e−03	3.27661960e−02	8.143e−03	8849	2.431e−03
90	3.10848873e−02	−9.742e−05	1183	4.571e−03	3.09688348e−02	3.636e−03	2425	3.733e−03	3.09688348e−02	3.636e−03	2425	0.000e+00
100	2.91721038e−02	1.422e−02	858	0.000e+00	2.91721038e−02	4.618e−04	858	0.000e+00	2.91721038e−02	4.618e−04	858	0.000e+00
Average		6.709e−04		4.000e−04		2.551e−04		1.723e−04		3.857e−04		3.712e−04

Table 3: Comparison of the best radii found for the problem "Sketch of America" when the initial guesses are random, like in [10], and when the proposed lattice-like initial guesses are considered.

another ball and an edge of the polygon simultaneously, or with a vertex of the polygon. Nonlinear systems formulated in this way may not have a single solution, regardless of whether the number of constraints is less than, equal to, or greater than the number of unknowns. Then, strategies for including different additional constraints can be explored. Figure 7 illustrates the idea. The figure corresponds to the solution found for an unitary-side equilateral triangle covered with $m = 6$ balls reported in Table 4. The points of contact in the figure were determined as follows. First, for each pair of balls we calculated the intersection points or determined that there were no intersection points. Let v be a point at the intersection of two balls. We checked if that point was on the boundary of the polygon or if it was on the boundary of a third ball. In these two verifications, we consider a tolerance of 10^{-4}. With the same precision, we checked if a vertex of the polygon was on the boundary of a ball. In the figure, the contact points are highlighted in colors: blue points lie in the intersection of three balls, green points are in the intersection of two balls and the polygon border, and yellow points are the points lying in the intersection of a ball with a polygon vertex. Red points are the centers of the balls. The constructed topology coincides with the one reported in [31, Fig.1]. In fact, in all cases except the squares with $m \in \{19, 28, 29\}$, i.e. 63 out of 66 instances, the topologies of the solutions found coincide with the ones reported in [31, 32], disregarding rotations and reflections. Additional details and topologies of all solutions found are available at `https://johngardenghi.github.io/bglcovering/`.

Having illustrated the proposed theoretical properties, the usefulness of the suggested initial points, and the fact that we found solutions matching those already known for small problems with triangles and squares, we now turn to the final experiment and report solutions with regular polygons and a larger number of balls. Regular triangles, squares, pentagons, hexagons, heptagons, octagons, nonagons, decagons, hendecagons, and dodecagons are considered. In all the cases the polygons are inscribed in a ball of unit radius. All polygons are covered with m balls with $m \in$

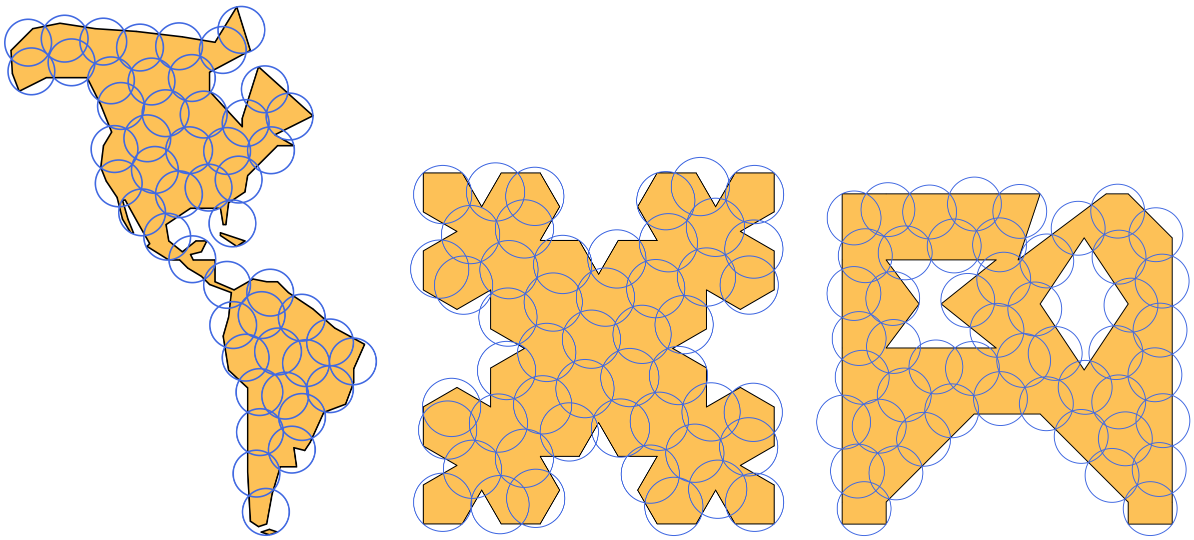

(a) $m = 50$

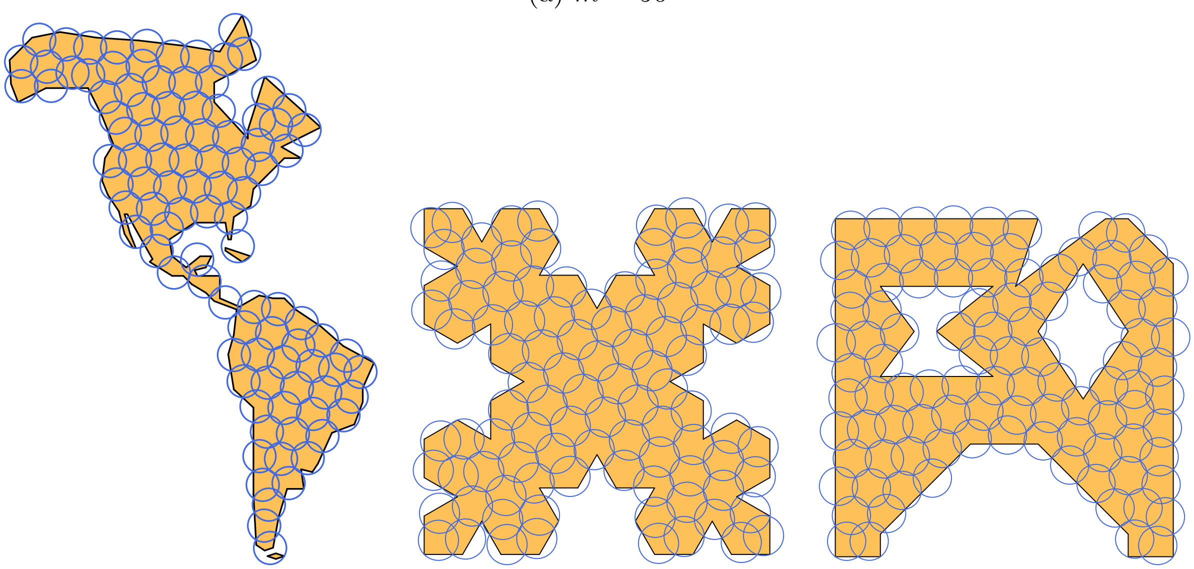

(b) $m = 100$

Figure 6: Illustration of some of the solutions found for the three problems in [10] considering a budget of $n_{\text{trials}} = 10\,000$ trials. In all cases, solutions are better than the ones found in [10].

$\{10, 20, \ldots, 100\}$. These solutions can be used as a reference for future work. Tables 5, 6, and 7 show the results. In the tables, for each value of m, r^* represents the best radius found, $G(\boldsymbol{x}^*, r^*)$ corresponds to the feasibility of the solution found, "trial" is the starting point for which the best radius was found, "outit" is the number of outer iterations of the augmented Lagrangian approach, "innit" is the total number of inner iterations (iterations needed to solve the augmented Lagrangian subproblems), $\#G$, $\#\nabla G$, and $\#\nabla^2 G$ are the number of evaluations of the constraint G and its first- and second-order derivatives, respectively, and "Time" is the CPU time in seconds.

m	Equilateral triangles [31]			
	r^*	$e_{\text{abs}}(r^*)$	$e_{\text{rel}}(r^*)$	trial
1	5.77280145e-01	7.012e-05	1.215e-04	1
2	4.99929876e-01	7.012e-05	1.402e-04	1
3	2.88644062e-01	3.107e-05	1.076e-04	1
4	2.67917424e-01	3.177e-05	1.186e-04	1
5	2.49964913e-01	3.509e-05	1.403e-04	1
6	1.92433472e-01	1.662e-05	8.635e-05	1
7	1.85233921e-01	1.716e-05	9.266e-05	1
8	1.76974424e-01	1.824e-05	1.031e-04	8
9	1.66646234e-01	2.043e-05	1.226e-04	18
10	1.44314629e-01	2.294e-05	1.589e-04	6580
11	1.41043082e-01	1.138e-05	8.065e-05	2
12	1.37311665e-01	1.195e-05	8.703e-05	7
13	1.32653114e-01	1.127e-05	8.497e-05	9
14	1.27504793e-01	1.159e-05	9.092e-05	30
15	1.15453819e-01	1.624e-05	1.406e-04	6778
16	1.13704316e-01	8.263e-06	7.266e-05	7
17	1.11384415e-01	9.895e-06	8.883e-05	9804
18	1.09101628e-01	7.317e-06	6.706e-05	74
19	1.06165942e-01	7.851e-06	7.395e-05	239
20	1.03219240e-01	7.979e-06	7.729e-05	149
21	9.62128149e-02	1.223e-05	1.271e-04	131
22	9.51708356e-02	6.399e-06	6.724e-05	120
23	9.37681323e-02	6.159e-06	6.568e-05	2
24	9.23477016e-02	6.436e-06	6.969e-05	2
25	9.06121327e-02	6.112e-06	6.745e-05	2963
26	8.87769570e-02	5.968e-06	6.722e-05	5419
27	8.68814406e-02	9.899e-06	1.139e-04	179
28	8.24689720e-02	9.638e-06	1.169e-04	7481
29	8.17960594e-02	8.754e-06	1.070e-04	128
30	8.08744935e-02	8.357e-06	1.033e-04	3
31	7.98887009e-02	8.544e-06	1.069e-04	90
32	7.88420764e-02	8.546e-06	1.084e-04	1545
33	7.76287349e-02	8.387e-06	1.080e-04	2872
34	7.63794431e-02	8.011e-06	1.049e-04	888
35	7.51525099e-02	7.945e-06	1.057e-04	61
36	7.21609144e-02	7.869e-06	1.090e-04	757

m	Squares [32]			
	r^*	$e_{\text{abs}}(r^*)$	$e_{\text{rel}}(r^*)$	trial
1	7.07056804e-01	4.998e-05	7.068e-05	52
2	5.58989521e-01	2.747e-05	4.915e-05	1
3	5.03873696e-01	1.741e-05	3.456e-05	1
4	3.53533297e-01	2.009e-05	5.683e-05	158
5	3.26140886e-01	1.970e-05	6.039e-05	1
6	2.98712470e-01	1.459e-05	4.885e-05	1
7	2.74278938e-01	1.295e-05	4.720e-05	6685
8	2.60287083e-01	1.302e-05	5.003e-05	1
9	2.30625095e-01	1.183e-05	5.130e-05	6547
10	2.18223057e-01	1.046e-05	4.791e-05	1
11	2.12505241e-01	1.078e-05	5.070e-05	497
12	2.02266887e-01	9.002e-06	4.451e-05	5
13	1.94302602e-01	9.769e-06	5.027e-05	1
14	1.85502119e-01	8.428e-06	4.543e-05	1
15	1.79653567e-01	8.193e-06	4.560e-05	9
16	1.69419853e-01	7.198e-06	4.249e-05	2
17	1.65673625e-01	7.304e-06	4.409e-05	4
18	1.60632604e-01	7.059e-06	4.395e-05	3167
19	1.58320209e-01	-4.782e-04	-3.030e-03	3792
20	1.52240763e-01	6.048e-06	3.973e-05	1
21	1.48947735e-01	6.055e-06	4.065e-05	1
22	1.43683119e-01	1.006e-05	7.000e-05	3723
23	1.41238706e-01	6.117e-06	4.330e-05	1
24	1.38293187e-01	9.697e-06	7.011e-05	6
25	1.33540006e-01	8.700e-06	6.515e-05	6
26	1.31756013e-01	8.863e-06	6.726e-05	625
27	1.28624755e-01	8.779e-06	6.825e-05	2984
28	1.27571769e-01	-2.542e-04	-1.997e-03	1923
29	1.25946556e-01	-3.930e-04	-3.131e-03	4
30	1.22029317e-01	7.552e-06	6.188e-05	1

Table 4: Comparison of the best radii found for the problem of covering an equilateral triangle and a square, both with side 1, when the algorithms in [31, 32] are considered and when the proposed lattice-like initial guesses are considered.

Figures 8, 9, and 10 illustrate the solutions found with $m \in \{10, 50, 100\}$, respectively. Additional details and topologies of all solutions found are available at `https://johngardenghi.github.io/bglcovering/`.

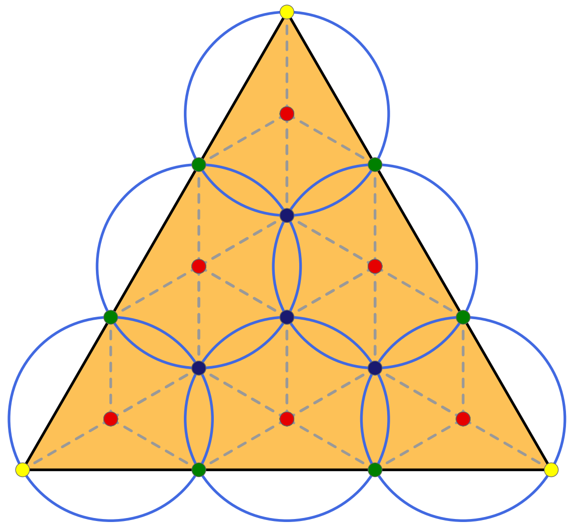

Figure 7: Example of how to assemble a nonlinear system by identifying the topology of a solution. In the example, a unitary-side equilateral triangle covered by $m = 6$ balls is considered. Red points correspond to the balls' centers, blue points lie in the intersection of three balls, green points are in the intersection of two balls and a triangle side, and yellow points are the points lying in the intersection of a ball with a triangle vertex.

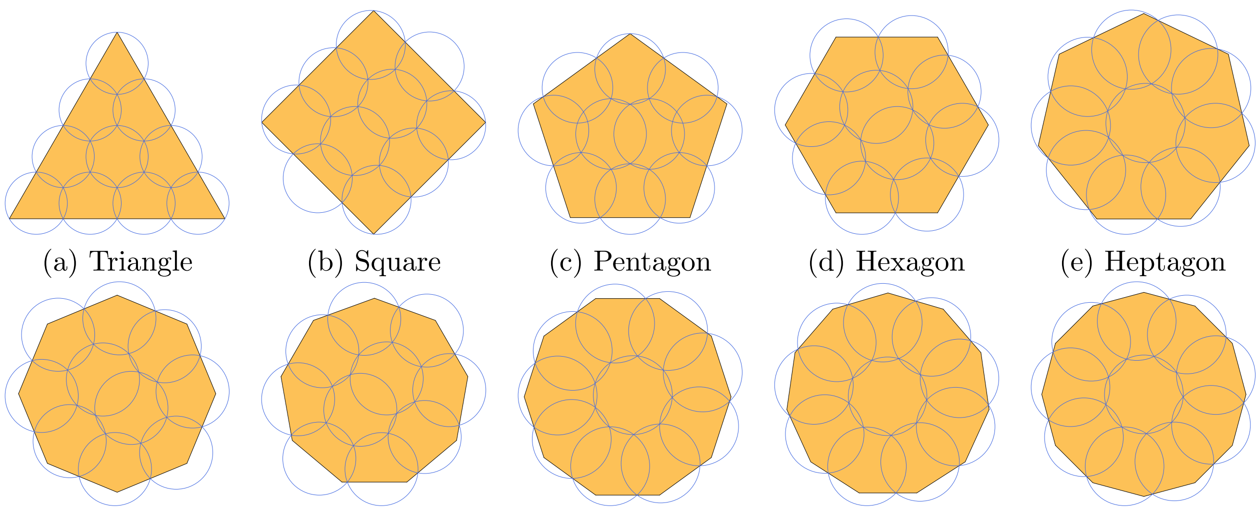

(a) Triangle (b) Square (c) Pentagon (d) Hexagon (e) Heptagon

(f) Octagon (g) Nonagon (h) Decagon (i) Hendecagon (j) Dodecagon

Figure 8: Illustration of the solution found for the problem of covering regular polygons with $m = 10$ balls.

6 Final considerations

The present work contributes to the study of lower and upper bounds on the optimal radius in the problem of covering a set with minimum radius identical balls, for a relatively large class

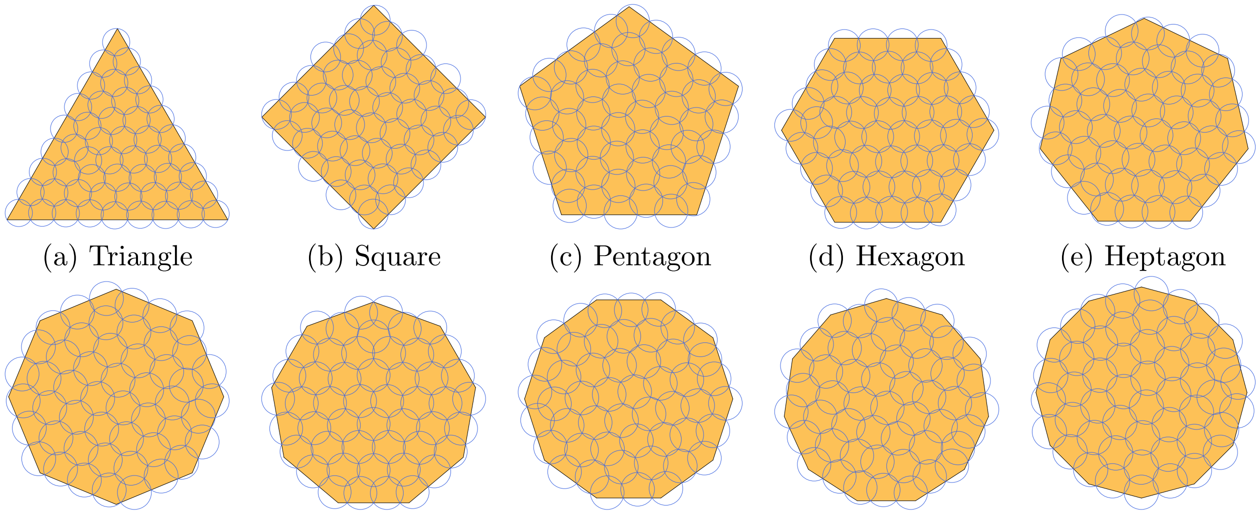

(a) Triangle (b) Square (c) Pentagon (d) Hexagon (e) Heptagon

(f) Octagon (g) Nonagon (h) Decagon (i) Hendecagon (j) Dodecagon

Figure 9: Illustration of the solution found for the problem of covering regular polygons with $m = 50$ balls.

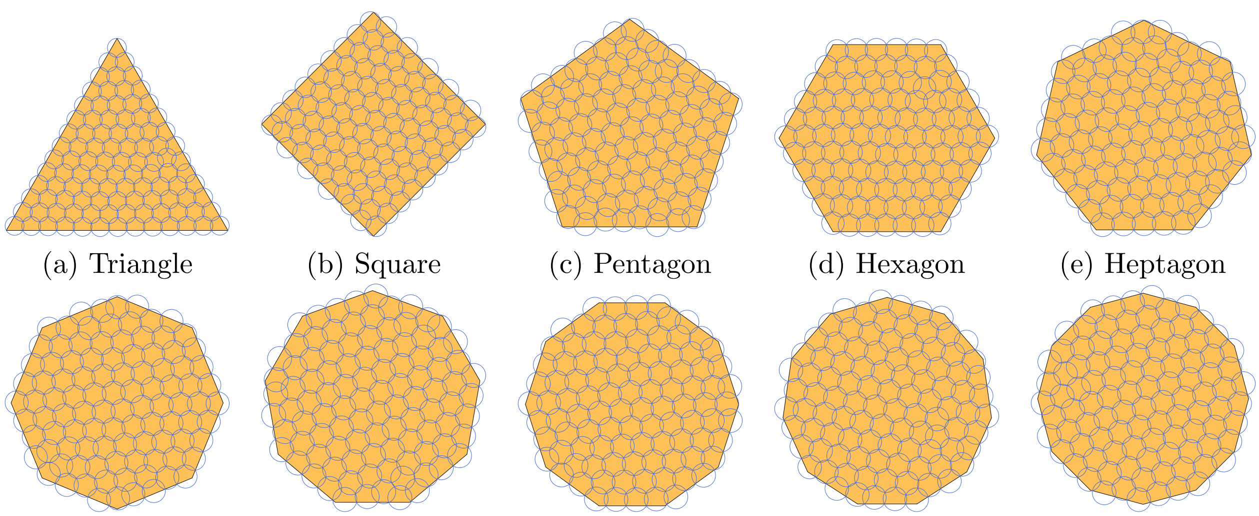

(a) Triangle (b) Square (c) Pentagon (d) Hexagon (e) Heptagon

(f) Octagon (g) Nonagon (h) Decagon (i) Hendecagon (j) Dodecagon

Figure 10: Illustration of the solution found for the problem of covering regular polygons with $m = 100$ balls.

of sets to be covered, and to its asymptotic analysis as the number m of balls goes to infinity. The asymptotic results of Kershner [24], in the problem of estimating the minimum number of identical discs of given radius r that is required to cover an arbitrary plane bounded set, are also discussed and compared with our main asymptotic expansion. This work is also a theoretical and numerical investigation of the relation between coverings based on regular hexagonal lattice arrangement, which are optimal when covering the whole plane, and covering of bounded sets with a finite number of balls. The regular hexagonal lattice arrangement is the key ingredient to obtain the asymptotic expansion of the optimal radius with respect to m, and is also the basis for the heuristic generation of initial guesses in our numerical experiments. Using these starting points, a multi-start optimization method was used to generate coverings of a wide range of regular polygons with up to 100 balls. Known results for triangles and squares were recovered and new results were presented.

Several lines for future research naturally arise for the continuation of this work. Assessing the sharpness of the bounds seems out of reach, as this would require to determine the precise asymptotic behaviour of the radius for a specific and most likely nonsmooth geometry. Thus, performing numerical experiments for specific geometries, as was done in the present work, seems to be the best way to gain insight on the general asymptotic behaviour of the radius, and to determine relevant objectives for future mathematical investigations.

Improving the bounds for a smaller class of shapes, such as polygons, seems to be a reasonable research objective. In the case of polygons, our numerical results indicate that the convergence rate for the lower bound could be improved, while the rate of the upper bound seems to be sharp, but the constant could be refined. Thus, there is some room for improvements in this particular case. Generalizing our approach to a larger class of sets to be covered would also be an interesting problem. In the case of arbitrary domains A, the asymptotic analysis of the radius could be achieved by covering tubular neighborhoods A_ε of A and let the parameter $\varepsilon \to 0$. This would require a more complex asymptotic analysis with two parameters ε and m.

From the methodological point of view, one could also try to refine the approach proposed in this paper. Since the asymptotic analysis is based on the inclusions $A_{-h} \subset H_1 \subset \overline{A}$ and $A \subset H_0 \subset \overline{A_h}$ where H_0, H_1 are honeycombs and A_h, A_{-h} converge to A as $h \to 0$, potential improvements of the estimates could be achieved by determining tighter inclusions. This would require a finer geometrical analysis of the behaviour of $\Omega(\boldsymbol{x}^*(m), r^*(m))$ in the neighborhood of ∂A.

References

[1] R. Andreani, E. G. Birgin, J. M. Martínez, and M. L. Schuverdt. On Augmented Lagrangian methods with general lower-level constraints. *SIAM Journal on Optimization*, 18(4):1286–1309, 2008.

[2] R. P. Bambah. On lattice coverings by spheres. *Proceedings of the National Institute of Sciences of India*, 20:25–52, 1954.

[3] R. P. Bambah and C. A. Rogers. Covering the planes with convex sets. *The Journal of the London Mathematical Society*, 27:304–314, 1952.

[4] R. P. Bambah and A. C. Woods. On plane coverings with convex domains. *Mathematika*, 18(1):91–97, 1971.

[5] B. Bánhelyi, E. Palatinus, and B. L. Lévai. Optimal circle covering problems and their applications. *Central European Journal of Operations Research*, 23(4):815–832, 2015.

[6] U. Betke, M. Henk, and J. M. Wills. A new approach to covering. *Mathematika*, 42(2):251–263, 1995.

[7] E. G. Birgin and J. M. Gentil. New and improved results for packing identical unitary radius circles within triangles. *Computers & Operations Research*, 37(7):1318–1327, 2010.

[8] E. G. Birgin, W. Gómez, G. Haeser, L. M. Mito, and D. S. Viana. An Augmented Lagrangian algorithm for nonlinear semidefinite programming applied to the covering problem. *Computational and Applied Mathematics*, 39(1):10, 2020.

[9] E. G. Birgin, A. Laurain, R. Massambone, and A. G. Santana. A shape optimization approach to the problem of covering a two-dimensional region with minimum-radius identical balls. *SIAM Journal on Scientific Computing*, 43(3):A2047–A2078, 2021.

[10] E. G. Birgin, A. Laurain, R. Massambone, and A. G. Santana. A shape-Newton approach to the problem of covering with identical balls. *SIAM Journal on Scientific Computing*, 44(2):A798–A824, 2022.

[11] E. G. Birgin and J. M. Martínez. *Practical Augmented Lagrangian Methods for Constrained Optimization.* Society for Industrial and Applied Mathematics, Philadelphia, PA, 2014.

[12] E. G. Birgin and J. M. Martínez. Complexity and performance of an Augmented Lagrangian algorithm. *Optimization Methods and Software*, 35(5):885–920, 2020.

[13] K. Böröczky, Jr. *Finite packing and covering.* Cambridge University Press, Cambridge, 2004.

[14] S. Cafieri, P. Hansen, and F. Messine. Global exact optimization for covering a rectangle with circles. *Journal of Global Optimization*, 2021.

[15] J. H. Conway and N. J. A. Sloane. *Sphere packings, lattices and groups.* Springer-Verlag, New York, NY, 3rd edition, 1999.

[16] G. K. Das, S. Das, S. C. Nandy, and B. P. Sinha. Efficient algorithm for placing a given number of base stations to cover a convex region. *Journal of Parallel and Distributed Computing*, 66(11):1353–1358, 2006.

[17] M. C. Delfour and J.-P. Zolésio. *Shapes and geometries: Metrics, analysis, differential calculus, and optimization.* Society for Industrial and Applied Mathematics, Philadelphia, PA, 2nd edition, 2011.

[18] I. Fáry. Sur la densité des réseaux de domaines convexes. *Bulletin de la Société Mathématique de France*, 78:152–161, 1950.

[19] L. Fejes Tóth. Eine bemerkung über die bedeckung der ebene durch eibereiche mit mittelpunkt. *Acta Scientiarum Mathematicarum*, 11(1–2):93–95, 1948.

[20] Sh. I. Galiev and M. A. Karpova. Optimization of multiple covering of a bounded set with circles. *Computational Mathematics and Mathematical Physics*, 50(4):721–732, 2010.

[21] A. Glazyrin. Covering a ball by smaller balls. *Discrete & Computational Geometry*, 62(4):781–787, 2019.

[22] A. Gray. *Tubes.* Springer Basel AG, Basel, Switzerland, 2nd edition, 2004.

[23] A. Henrot and M. Pierre. *Shape variation and optimization.* European Mathematical Society, Zürich, 2018.

[24] R. Kershner. The number of circles covering a set. *American Journal of Mathematics*, 61(3):665–671, 1939.

[25] A. Laurain. Distributed and boundary expressions of first and second order shape derivatives in nonsmooth domains. *Journal de Mathématiques Pures et Appliquées*, 134:328–368, 2020.

[26] A. Laurain and K. Sturm. Distributed shape derivative *via* averaged adjoint method and applications. *ESAIM: Mathematical Modelling and Numerical Analysis*, 50(4):1241–1267, 2016.

[27] H. Melissen. Loosest circle coverings of an equilateral triangle. *Mathematics Magazine*, 70(2):118–124, 1997.

[28] J. B. M. Melissen and P. C. Schuur. Improved coverings of a square with six and eight equal circles. *The Electronic Journal of Combinatorics*, 3:R32, 1996.

[29] J. B. M. Melissen and P. C. Schuur. Covering a rectangle with six and seven circles. *Discrete Applied Mathematics*, 99(1–3):149–156, 2000.

[30] E. H. Neville. On the solution of numerical functional equations: Illustrated by an account of a popular puzzle and of its solution. *Proceedings of the London Mathematical Society*, s2-14(1):308–326, 01 1915.

[31] K. J. Nurmela. Conjecturally optimal coverings of an equilateral triangle with up to 36 equal circles. *Experimental Mathematics*, 9(2):241–250, 2000.

[32] K. J. Nurmela and P. R. J. Östergärd. Covering a square with up to 30 equal circles. Technical Report Technical Report HUT-TCS-A62, Helsinki University of Technology, 2000.

[33] J. Sokolowski and J.-P. Zolesio. Introduction to shape optimization. In *Introduction to Shape Optimization: Shape Sensitivity Analysis*, pages 5–12. Springer Berlin Heidelberg, Berlin, Heidelberg, 1992.

[34] Y. G. Stoyan and V. M. Patsuk. Covering a compact polygonal set by identical circles. *Computational Optimization and Applications*, 46(1):75–92, 2010.

[35] I. E. Sutherland and G. W. Hodgman. Reentrant polygon clipping. *Association for Computing Machinery*, 17(1):32–42, 1974.

[36] T. Tarnai and Zs. Gáspár. Covering a square by equal circles. *Elemente der Mathematik*, 50(4):167–170, 1995.

[37] S. Verblunsky. On the least number of unit circles which can cover a square. *Journal of the London Mathematical Society*, s1-24(3):164–170, 1949.

[38] J.-L. Verger-Gaugry. Covering a ball with smaller equal balls in $\mathbb{R}^n$. *Discrete & Computational Geometry*, 33(1):143–155, 2005.

[39] Z. T. Zahn Jr. Black-box maximization of circular coverage. *Journal of Research of National Bureau of Standards B, Mathematics and Mathematical Physics*, 66B(4):181–216, 1962.

[40] C. Zong. Packing, covering and tiling in two-dimensional spaces. *Expositiones Mathematicae*, 32(4):297–364, 2014.

	m	r^*	$G(\boldsymbol{x}^*, r^*)$	trial	outit	innit	$\#G$	$\#\nabla G$	$\#\nabla^2 G$	Time
Triangle	10	2.49977020e-01	9.2e-09	5510	24	297	4878	499	537	0.15
	20	1.78786808e-01	4.1e-09	149	23	178	1641	396	408	0.21
	30	1.40084849e-01	9.3e-09	92	22	162	1576	376	382	0.31
	40	1.20685149e-01	8.4e-09	416	21	150	1497	358	360	0.42
	50	1.07098025e-01	7.7e-09	653	21	169	1793	375	379	0.90
	60	9.69870980e-02	7.0e-09	1	21	176	2033	368	386	0.89
	70	8.91183837e-02	1.0e-08	1806	21	151	1440	351	361	0.97
	80	8.27428405e-02	9.7e-09	1186	23	167	1646	398	397	1.21
	90	7.81891689e-02	9.8e-09	124	22	154	1608	361	374	1.29
	100	7.40088440e-02	9.4e-09	1047	21	150	1093	351	360	0.90
Square	10	3.08571384e-01	6.6e-09	2565	24	187	1520	369	427	0.08
	20	2.15303457e-01	3.5e-09	1	22	106	325	320	326	0.09
	30	1.72578643e-01	8.8e-09	1	21	98	303	299	308	0.14
	40	1.49691784e-01	8.4e-09	52	19	95	285	279	285	0.20
	50	1.33506224e-01	7.8e-09	845	21	104	324	310	314	0.27
	60	1.19278125e-01	7.2e-09	2	22	117	347	333	337	0.36
	70	1.10734524e-01	6.7e-09	10	23	125	528	350	355	0.57
	80	1.03299126e-01	9.7e-09	4	20	94	291	287	294	0.46
	90	9.64117309e-02	9.3e-09	2	21	108	325	315	318	0.51
	100	9.18362926e-02	9.1e-09	11	20	100	318	298	300	0.41
Pentagon	10	3.47157834e-01	4.8e-09	7	21	102	311	300	312	0.04
	20	2.36699399e-01	3.8e-09	6038	22	115	340	331	335	0.11
	30	1.89454524e-01	9.9e-09	1776	21	158	1182	362	368	0.27
	40	1.62502626e-01	8.3e-09	19	21	105	333	315	315	0.22
	50	1.45008700e-01	7.8e-09	4506	23	176	1681	395	406	0.66
	60	1.31534995e-01	7.3e-09	8	21	107	324	314	317	0.37
	70	1.21114143e-01	7.0e-09	1151	20	113	429	302	313	0.46
	80	1.13185579e-01	6.7e-09	1623	19	96	285	280	286	0.47
	90	1.06318158e-01	1.0e-08	36	20	108	312	304	308	0.63
	100	1.00531052e-01	9.6e-09	7294	21	104	315	308	314	0.52
Hexagon	10	3.60385567e-01	5.2e-09	1	22	104	329	319	324	0.05
	20	2.42926722e-01	4.0e-09	32	22	125	378	343	345	0.11
	30	1.96015058e-01	9.5e-09	3	21	103	321	309	313	0.14
	40	1.68398394e-01	8.6e-09	534	22	181	1758	392	401	0.51
	50	1.50160811e-01	7.8e-09	5821	21	140	800	337	350	0.47
	60	1.36428612e-01	7.3e-09	4525	21	157	1129	362	367	0.67
	70	1.24733832e-01	6.7e-09	1	23	223	1746	368	453	0.74
	80	1.16368899e-01	9.7e-09	1	21	104	332	306	314	0.50
	90	1.10098066e-01	9.7e-09	121	23	164	1630	389	394	1.39
	100	1.04220865e-01	9.4e-09	4264	22	183	1941	393	403	1.36

Table 5: Details of the solutions obtained for the problem (1,2) for regular polygons by the application of Algencan.

	m	r^*	$G(\boldsymbol{x}^*, r^*)$	trial	outit	innit	$\#G$	$\#\nabla G$	$\#\nabla^2 G$	Time
Heptagon	10	3.66674709e-01	4.5e-09	9774	22	119	358	337	339	0.05
	20	2.52023120e-01	4.0e-09	2229	22	129	384	353	349	0.12
	30	2.03987279e-01	9.6e-09	4115	21	166	1489	354	376	0.32
	40	1.74410069e-01	8.6e-09	269	21	195	1547	404	405	0.48
	50	1.54316526e-01	7.7e-09	2	22	109	332	324	329	0.25
	60	1.40423516e-01	7.3e-09	197	21	100	312	306	310	0.35
	70	1.29459571e-01	6.8e-09	10	21	125	522	334	335	0.46
	80	1.20693169e-01	9.9e-09	1753	22	177	1821	396	397	1.32
	90	1.13890081e-01	1.0e-08	625	22	157	1400	369	377	1.28
	100	1.07573511e-01	9.4e-09	676	18	93	275	268	273	0.45
Octagon	10	3.71068736e-01	5.1e-09	1	22	108	329	323	328	0.07
	20	2.55463469e-01	3.9e-09	1	23	138	411	370	368	0.10
	30	2.05300348e-01	9.7e-09	1	21	98	307	303	308	0.13
	40	1.78141373e-01	8.6e-09	1306	21	163	1723	363	373	0.41
	50	1.57924226e-01	7.9e-09	4665	22	160	1429	365	380	0.49
	60	1.42441662e-01	7.3e-09	3251	19	102	317	289	292	0.32
	70	1.31887850e-01	6.7e-09	632	22	116	351	328	336	0.42
	80	1.23510395e-01	9.7e-09	1546	22	129	518	347	349	0.57
	90	1.15333106e-01	9.6e-09	7555	21	142	1093	346	352	0.94
	100	1.09342373e-01	9.7e-09	2939	22	164	1640	373	384	0.99
Nonagon	10	3.85176628e-01	5.2e-09	1	22	106	334	322	326	0.04
	20	2.59174664e-01	3.9e-09	1515	22	143	421	370	363	0.12
	30	2.12497351e-01	9.7e-09	1066	20	147	1018	356	347	0.25
	40	1.80612723e-01	8.6e-09	90	23	193	1930	412	423	0.54
	50	1.59353027e-01	8.0e-09	34	23	174	1712	401	404	0.65
	60	1.44330783e-01	7.3e-09	293	19	99	293	285	289	0.31
	70	1.33242038e-01	7.1e-09	215	21	115	344	321	325	0.46
	80	1.24487543e-01	9.8e-09	629	22	150	1350	364	370	1.04
	90	1.17022226e-01	1.0e-08	6086	21	143	1128	349	353	1.10
	100	1.10619955e-01	9.6e-09	6878	20	164	1796	358	364	1.20
Decagon	10	3.81588699e-01	4.4e-09	918	23	129	397	361	359	0.06
	20	2.61419395e-01	4.0e-09	601	24	146	552	389	386	0.13
	30	2.14184123e-01	9.5e-09	4884	21	158	1290	355	368	0.30
	40	1.83010882e-01	8.6e-09	538	21	162	1443	362	372	0.45
	50	1.61812154e-01	7.8e-09	7432	22	173	1352	388	393	0.57
	60	1.45272987e-01	7.2e-09	58	19	95	301	279	285	0.36
	70	1.34006026e-01	6.7e-09	1924	21	115	353	320	325	0.50
	80	1.25791279e-01	9.7e-09	685	21	144	1136	347	354	0.97
	90	1.17869397e-01	9.8e-09	3498	21	148	1025	358	358	1.15
	100	1.11744936e-01	9.6e-09	9	22	200	2498	414	420	1.56

Table 6: Details of the solutions obtained for the problem (1,2) for regular polygons by the application of Algencan.

	m	r^*	$G(\boldsymbol{x}^*, r^*)$	trial	outit	innit	$\#G$	$\#\nabla G$	$\#\nabla^2 G$	Time
Hendecagon	10	3.84661357e-01	4.4e-09	9710	22	120	372	339	340	0.05
	20	2.62677708e-01	4.0e-09	922	24	165	708	407	405	0.15
	30	2.15250896e-01	9.5e-09	1304	21	184	1948	394	394	0.38
	40	1.84173758e-01	8.5e-09	31	21	148	944	348	358	0.37
	50	1.62219728e-01	7.6e-09	4509	21	111	339	311	321	0.30
	60	1.46310501e-01	7.3e-09	631	21	101	318	305	311	0.35
	70	1.35416461e-01	6.9e-09	2819	21	111	337	321	321	0.48
	80	1.26395606e-01	9.9e-09	3588	21	134	958	339	344	0.91
	90	1.18066734e-01	9.7e-09	9620	20	107	348	313	307	0.63
	100	1.12183055e-01	9.6e-09	5008	20	132	569	329	332	0.65
Dodecagon	10	3.85525578e-01	4.3e-09	1928	24	142	666	378	382	0.07
	20	2.62857990e-01	4.0e-09	419	22	129	382	344	349	0.12
	30	2.16895193e-01	9.7e-09	772	21	143	924	350	353	0.26
	40	1.84703019e-01	8.4e-09	5	21	111	342	318	321	0.23
	50	1.63143643e-01	7.9e-09	3169	21	173	1828	381	383	0.68
	60	1.46500536e-01	7.3e-09	408	19	105	311	292	295	0.35
	70	1.35802478e-01	6.8e-09	1	21	113	335	317	323	0.38
	80	1.26683441e-01	9.5e-09	1487	22	159	1416	366	379	0.91
	90	1.18806744e-01	9.8e-09	26	18	90	281	267	270	0.54
	100	1.12616779e-01	9.3e-09	52	18	100	302	278	280	0.50

Table 7: Details of the solutions obtained for the problem (1,2) for regular polygons by the application of Algencan.